

Vanadian and chromian garnet- and epidote-supergroup minerals in metamorphosed Paleozoic black shales from Čierna Lehota, Strážovské vrchy Mountains, Slovakia: crystal chemistry and evolution

PETER BAČÍK^{1,*}, PAVEL UHER¹, PETRA KOZÁKOVÁ¹, MARTIN ŠTEVKO¹, DANIEL OZDÍN¹ AND TOMÁŠ VACULOVÍČ²

¹ Comenius University in Bratislava, Faculty of Natural Sciences, Department of Mineralogy and Petrology, Ilkovičova 6, 842 15 Bratislava, Slovak Republic

² Masaryk University, Faculty of Science, Department of Chemistry, Kotlářská 2, 611 37 Brno, Czech Republic

[Received 24 December 2016; Accepted 25 July 2017; Associate Editor: Ed Grew]

Abstract

Silicate minerals enriched in V, Cr and Mn including garnets and epidote-supergroup members, in association with amphiboles, albite, hyalophane, titanite, chamosite, sulfides and other minerals occur in Devonian black shales near Čierna Lehota in the Strážovské vrchy Mountains, Slovakia. The garnets have high concentrations of V, Cr and Mn (up to 17 wt.% V₂O₃, ≤11 wt.% Cr₂O₃ and ≤21 wt.% MnO) and several compositional types. Vanadian-chromian grossular (Grs 1) usually preserves primary metamorphic oscillatory zoning, whereas solid solutions between goldmanite (Gld 2A,B), V- and Cr-rich grossular and spessartine (Grs 2A,B, Sps 2) form irregular domains or crystals with variable zoning. Dominant substitutions in the garnets include CaMn₋₁ and (V,Cr)Al₋₁, resulting in coupled Ca(V,Cr)Mn₋₁Al₋₁. Epidote-supergroup minerals occur as abundant anhedral crystals with variable compositional zoning. Nearly all crystals have a complete zoning sequence beginning with REE-rich allanite-(La), followed by mukhinite and by V- and Cr-rich clinozoisite to mukhinite and V- and Cr-poor clinozoisite. In common with garnets, the epidote-supergroup minerals are enriched in V, Cr and Mn (<7 wt.% V₂O₃, <5 wt.% Cr₂O₃ and <3 wt.% MnO). Lanthanum is the dominant REE (up to 11.5 wt.% La₂O₃) in allanite-(La). The composition of epidote-supergroup minerals is controlled by REEFe²⁺(CaAl)₋₁, REEMg(CaAl)₋₁, REEMn²⁺(CaAl)₋₁ and REEFe²⁺(CaFe³⁺)₋₁ substitutions introducing REE, together with VAl₋₁ and CrAl₋₁ substitutions. The negative Ce and slightly positive Eu anomalies displayed in chondrite-normalized patterns and enrichment in V, Cr and Mn are ascribed to the geochemical properties of the protolith. The minerals investigated exhibit multi-stage evolution: (1) presumed low-grade greenschist-facies metamorphism; and (2) development of V- and Cr-rich zones in both garnet- and epidote-supergroup minerals which result from late-Variscan contact metamorphism due to granitic intrusion of the Suchý Massif. Decreased temperature following the metamorphic peak probably resulted in the formation of REE-, V- and Cr-poor clinozoisite and secondary garnet.

KEYWORDS: garnet supergroup, goldmanite, epidote supergroup, mukhinite, allanite-(La), black shales, Čierna Lehota, Western Carpathians, Slovakia.

Introduction

SILICATE and oxide minerals containing essential V are relatively uncommon. They were found in vanadium-rich calcareous metapelites-metapsammites, metacherts, marbles, skarns and metapyroclastic rocks, usually enriched in calcium,

*E-mail: peter.bacik@uniba.sk

<https://doi.org/10.1180/minmag.2017.081.068>

sulfur and organic carbonaceous matter, and commonly found in contact metamorphic aureoles associated with magmatic rocks. The vanadium-rich metamorphic mineral assemblage consists of garnets (V-rich grossular to goldmanite), commonly found together with other V-rich silicate minerals: members of the epidote supergroup, mica supergroup, pyroxene group, amphibole supergroup and titanite and other phases (as in Moench and Meyrowitz, 1964; Shepel and Karpenko, 1969; Karev, 1974; Litochleb *et al.*, 1985, 1997; Benkerrou and Fonteilles, 1989; Osanai *et al.*, 1990; Pan and Fleet, 1991; Jeong and Kim, 1999). Rarely, the V-rich silicate minerals are also notably enriched in Cr³⁺ (Filippovskaya *et al.*, 1972; Uher *et al.*, 1994, 2008; Secco *et al.*, 2002; Canet *et al.*, 2003; Makrygina *et al.*, 2004). Moreover, a specific compositional group is represented by manganovanadian garnets, including Mn,V-rich grossular–V-rich spessartine–momoiite (Mn₃V₂Si₃O₁₂)–Mn-rich goldmanite solid solution (Momoi, 1964; Kato *et al.*, 1994; Černý *et al.*, 1995; Tanaka *et al.*, 2010; Matsubara *et al.*, 2010).

In this work, we describe a new occurrence of vanadium-rich garnet- and epidote-supergroup minerals in amphibole-rich metasediments with organic matter (black shales) near Čierna Lehota village in the Strážovské vrchy Mountains, Western Carpathians (Western Slovakia). This V-Cr silicate mineralization in black shales is related closely to the syngenetic metamorphic pyrite-pyrrhotite and younger hydrothermal Ni–Bi–As sulfide mineralization described in earlier works (Mikuš *et al.*, 2013; Pršek *et al.*, 2005). The V- and Cr-enriched silicate mineralization at Čierna Lehota has geological and mineralogical similarities to previously described metamorphic V- and Cr-rich silicate assemblage from the Pezinok area in the Malé Karpaty Mountains in south-western Slovakia (Uher *et al.*, 1994, 2008; Bačík and Uher, 2010). Both occurrences are located in Lower Paleozoic (Devonian) metamorphosed, deep-marine carbonaceous volcano-sedimentary rocks related to ophiolites; the silicate minerals in these metasediments have significant V and Cr enrichment.

The garnet- and epidote-supergroup minerals from Čierna Lehota reveal a uniquely complex V, Cr,±Mn and REE enrichment not previously reported in the global occurrences mentioned above. The objective of this paper is description of the crystal chemistry, compositional zoning and substitutions of V- and Cr-rich members of garnet and epidote-supergroup minerals from the Čierna Lehota occurrence. On the basis of crystal chemistry and zoning, we propose a

genetic model for the evolution of these minerals and discuss their similarities and differences with comparable occurrences.

Geological setting

The occurrence of vanadian-chromian and sulfide mineralization investigated is situated 2 km SSE of Čierna Lehota village in the Strážovské vrchy Mountains, western Slovakia (Fig. 1). The Strážovské vrchy Mountains are part of the Tatric Superunit of the Central Western Carpathians (Plašienka *et al.*, 1997) and they form part of the Tatra–Fatra Belt comprising the Tatric pre-Alpine, Lower Paleozoic crystalline basement and its Late Paleozoic to Mesozoic sedimentary cover (Plašienka *et al.*, 1997). Together with the Vepor belt, the Tatra–Fatra Belt forms the inner Variscan zone of the Central Western Carpathians basement complexes. These contain medium- to high-grade metamorphic rocks and abundant granitic plutons.

The pre-Alpine Suchý–Malá Magura crystalline basement in the Strážovské Mountains consists of granitic rocks, migmatites, metapelites to metapsammites, amphibolites, schists and granitic rocks (Kahan, 1979, 1980; Hrouda *et al.*, 1983; Mahel', 1986; Hovorka and Méres, 1991; Krist *et al.*, 1992 and references therein). The metamorphosed sedimentary rocks represented by Lower Paleozoic gneisses, graphitic metasediments and metacherts underwent Variscan regional and contact metamorphism under greenschist- to amphibolite-facies conditions at ~300–500 MPa and 460–700°C (Korikovsky *et al.*, 1984; Vilinovičová, 1990; Hovorka and Méres, 1991; Krist *et al.*, 1992; Dyda, 1994). The Suchý–Malá Magura crystalline complex is intruded by meso-Variscan (~350 Ma, Král' *et al.*, 1997; Finger *et al.*, 2003) peraluminous, garnet-bearing granitic rocks with S-type affinity (Hovorka and Fejdi, 1983; Vilinovičová, 1990; Broska and Uher, 2001).

The host rocks of syngenetic pyrite and pyrrhotite and associated V-Cr-rich silicate mineralization are Lower Paleozoic, and probably Devonian, metamorphosed black shales, mainly gneisses, metaquartzites (metacherts), amphibole schists and amphibolites. The samples investigated are metabasic rocks (amphibolites to amphibole schists) with abundant disseminated sulfide mineralization consisting mainly of pyrite (euhedral cubic crystals up to 1 cm or anhedral aggregates up to several cm) and pyrrhotite (anhedral grains and irregular aggregates up to 4 cm) and also minor

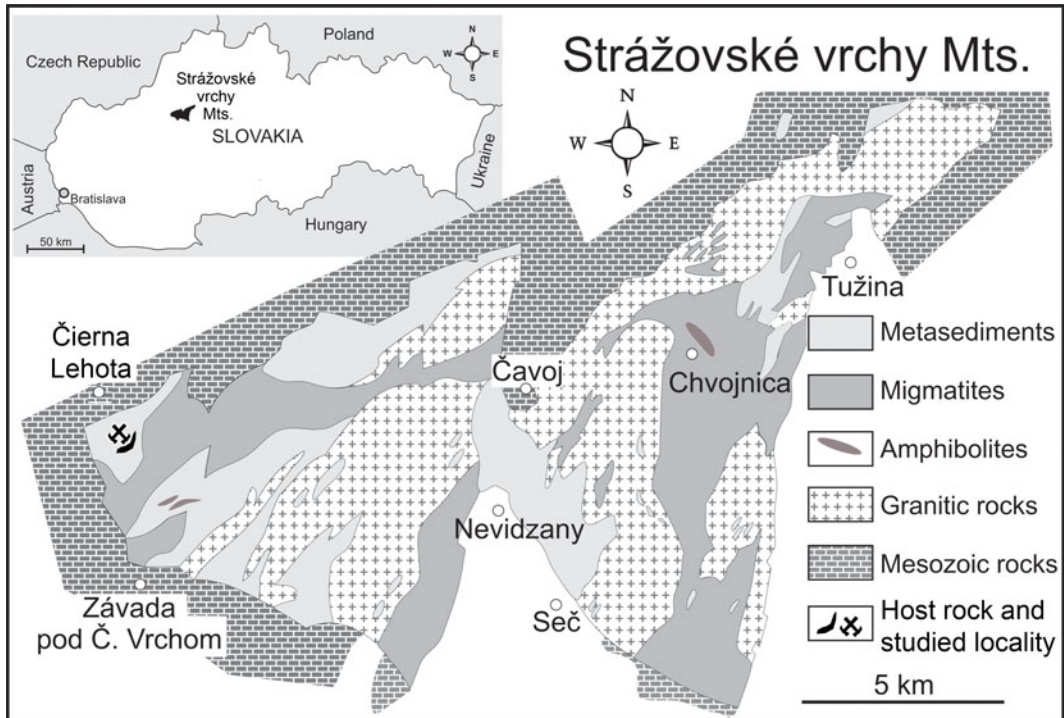


FIG. 1. Simplified geological map of the Strážovské vrchy Mountains showing the area of this investigation (modified after Maheľ *et al.* 1982)

sphalerite and galena (both as anhedral grains and aggregates up to 1 cm). The mineralized black shales and metabasic rocks form a narrow, ~20 m thick zone trending SSW–NNE in biotite paragneisses of the Suchý–Malá Magura crystalline complex (Mikuš *et al.*, 2013). The layers of basic amphibolite and amphibolite schist metavolcanic rocks and the associated carbon- and silica-rich oceanic sediments (black shales) deposited in anoxic conditions are remnants of an Upper Devonian oceanic ophiolite sequence in the Suchý–Malá Magura crystalline complex. They are presumed to be part of the Pernek Group of tectonic relicts of Variscan ophiolite in a suture created by oceanic closure in the Lower Carboniferous and then preserved in the Malé Karpaty and Suchý–Malá Magura crystalline basements (Ivan and Méres, 2015).

Analytical methods

The composition of garnets and epidote-supergroup minerals was determined using a

CAMECA SX100 electron microprobe analyser (EMPA) in wavelength-dispersive spectrometric (WDS) mode (State Geological Institute of Dionýz Štúr, Bratislava), using the following analytical conditions: accelerating voltage 15 kV, beam current 20 nA and beam diameter 2 to 5 μm . The following standards were used: wollastonite ($\text{SiK}\alpha$, $\text{CaK}\alpha$), TiO_2 ($\text{TiK}\alpha$), ThO_2 ($\text{ThM}\alpha$), UO_2 ($\text{UM}\alpha$), Al_2O_3 ($\text{AlK}\alpha$), pure V ($\text{VK}\alpha$), pure Cr ($\text{CrK}\alpha$), synthetic phosphates of La-Lu and Y ($\text{REEL}\alpha$), fayalite ($\text{FeK}\alpha$), rhodonite ($\text{MnK}\alpha$), pure Ni ($\text{NiK}\alpha$), forsterite ($\text{MgK}\alpha$), SrTiO_3 ($\text{SrK}\alpha$), baryte ($\text{BaK}\alpha$), albite ($\text{NaK}\alpha$), orthoclase ($\text{KK}\alpha$), LiF ($\text{FK}\alpha$) and NaCl ($\text{ClK}\alpha$). Numerous interferences are present in the spectral lines of the measured elements, which were chosen to eliminate or at least minimize overlap. Empirical correction factors were applied where overlap persisted, and these were resolved for $\text{PbM}\alpha$ – $\text{YLa}\gamma_{2,3}$ and $\text{ThM}\zeta_{1,2}$, $\text{UM}\beta$ – $\text{ThM}\gamma$, ThM_3 and ThN_4 , $\text{UM}\beta$ – $\text{K}\alpha$, $\text{GdLa}\alpha$ – $\text{CeL}\chi$, $\text{GdLa}\alpha$ – LaLa , $\text{L}\chi_{2,3}$, $\text{GdLa}\alpha$ – $\text{NdL}\beta_2$, $\text{LuL}\beta$ – $\text{DyL}\chi_{2,3}$, $\text{HoL}\chi$ and $\text{YbL}\beta_2$, $\text{EuL}\beta$ – $\text{DyL}\nu$, $\text{FeK}\alpha$ and $\text{MnK}\beta$, $\text{ErL}\beta$ – $\text{EuL}\chi_{2,3}$, $\text{GdL}\chi$ and $\text{LuL}\nu$, $\text{SmLa}\alpha$ – $\text{CeL}\beta_2$, $\text{TmLa}\alpha$ – $\text{SmL}\chi$, $\text{FK}\alpha$ – $\text{CeM}\zeta_{1,3}$,

$FK\alpha$ – $MnL\beta$ and $FK\alpha$ – $FeL\alpha$ (Konečný *et al.*, 2004; Uher *et al.*, 2015). The averaged 20 nA detection limits for REE-bearing minerals with their concentrations in ppm are as follows: S 150; Si 430; Ti 390; Th 410; U 660; Al 350; Cr 360; V 520; Y 640; La 880; Ce 750; Pr 800; Nd 685; Sm 730; Eu 940; Tb 940; Dy 1030; Ho 1180; Er 1380; Tm 1090; Yb 980; Lu 2210; Fe 550; Mn 450; Mg 390; Ca 190; Sr 550; Ba 420; Pb 470; Na 450; K 180; F 380; and Cl 190. The standard deviations ($\pm\sigma$) vary between 0.02 and 0.3 wt.%, depending on the specific element concentration and peak measurement time between 10 and 90 s. Data were reduced with the PAP correction.

The structural formulae of garnet-supergroup minerals; $\{X_3\}[Y_2](Z_3)\phi_{12}$, were calculated based on eight cations (Grew *et al.*, 2013), and the epidote-supergroup minerals, $A_2M_3[T_2O_7][TO_4](O, F)(OH, O)$, were normalized based on $\Sigma(A + M + T) = 8$ cations and the Armbruster *et al.* (2006) procedure.

Instrumentation for laser ablation inductively coupled plasma mass spectrometry (LA-ICP-MS) analysis comprised the UP 213 laser ablation system (New Wave, USA) and the Agilent 7500 CE ICP-MS spectrometer (Agilent, Japan) at the Department of Chemistry, Masaryk University, Brno. A commercial Q-switched Nd-YAG laser ablation device working at the 5th harmonic frequency; corresponding to a 213 nm wavelength. The ablation device is equipped with a programable XYZ-stage to move the sample along a programed trajectory during ablation. Visual inspection and photographic documentation of analytical targets were accomplished with a built-in microscope/CCD-camera system.

The ablation cell was flushed with helium carrier gas to transport the laser-induced aerosol to the inductively coupled plasma (1.0 l/min), and a sample 0.6 l/min argon gas flow was mixed with the helium carrier gas flow behind the laser ablation cell. LA-ICP-MS conditions of gas flow rates, sampling depth and MS electrostatic lens voltage were optimized with NIST SRM 612 glass reference material to ensure maximum signal-to-noise ratio and minimum oxide formation (ThO⁺/Th⁺ counts ratio 0.2%, U⁺/Th⁺ counts ratio 1.1%). Hole drilling mode with fixed sample position during laser ablation was used for 40s for each spot; with 65 μm diameter (samples TSW), 13 J cm⁻² laser fluence and 10 Hz. repetition rate. All element contents obtained by LA-ICP-MS measurement were normalized using Si as the internal standard.

Results

Garnet-supergroup minerals

Garnets from Čierna Lehota form euhedral to subhedral isolated crystals up to 1 mm in size, and quite commonly, anhedral atoll-like overgrowths and aggregates ≤ 3 mm across (Fig. 2). Garnets have wide compositional range, especially in V, Cr and Al at the Y site, and Ca and Mn at the X site. Textural and compositional features indicated that there are two generations, G1 and G2, and five types of garnets (Table 1, Figs 2, 3a–b) in this study: V-Cr-rich grossular (Grs 1); goldmanite (Gld 2A) with highest V; Cr-rich goldmanite (Gld 2B) with lower V; V-Cr-rich grossular (Grs 2A); and solid solutions between Mn-rich grossular and spessartine (Grs-Sps 2B). The Grs1 garnet forms crystals with oscillatory zoning or relatively homogeneous grains and overgrowths on plagioclase (Fig. 2a–c), whereas the other garnet types have irregular patchy zoning or they are unzoned (Fig. 2b,d). Textural patterns indicate the primary and older origin of generation 1 (Grs 1), and the other four garnet types form the secondary and younger generation 2 (Gld 2A, Gld 2B, Grs 1A and Grs-Sps 2B).

Each garnet type exhibits a specific composition (Table 1). The primary Grs 1 grossular is V-Cr and Mn-rich and contains 0.34–0.55 atoms per formula unit (apfu) V, 0.22–0.34 apfu Cr and 0.88–1.20 apfu Mn; ⁵⁷Al varies between 1.1 and 1.3 apfu. Chromium-rich (0.51–0.59 apfu Cr) goldmanite Gld 2A has the highest V content (1.1 apfu) but lower ⁵⁷Al (0.3 to 0.4 apfu) and Mn (0.22–0.26 apfu) contents. The Gld 2B goldmanite exhibits highest Cr (0.51–0.70 apfu) and slightly lower V (0.8–0.9 apfu) contents but elevated ⁵⁷Al (0.4 to 0.7 apfu) and Mn (0.29–0.65 apfu) concentrations. Grossular Grs 2A is V- and Cr-rich (0.53–0.69 apfu V, 0.40–0.49 apfu Cr) but has medium Mn concentrations (0.38–0.71 apfu) and lower ⁵⁷Al (0.8 to 1.0 apfu). Grossular–spessartine solid solution Grs-Sps 2B exhibits the lowest V and Cr concentrations (0.01–0.35 apfu V and 0.003–0.19 apfu Cr) but the highest contents of Mn (0.56–1.42 apfu) and also ⁵⁷Al (1.4–2.0 apfu).

Magnesium content is generally low in all garnet types; reaching a maximum of 0.10 apfu Mg in Grs 2A and Grs-Sps 2B. Garnet Fe concentrations are relatively low with maximum of 0.3 apfu (Fe³⁺ + Fe²⁺) in V-Cr-poor garnets; intermediate between grossular and spessartine in composition (Grs-Sps 2B).

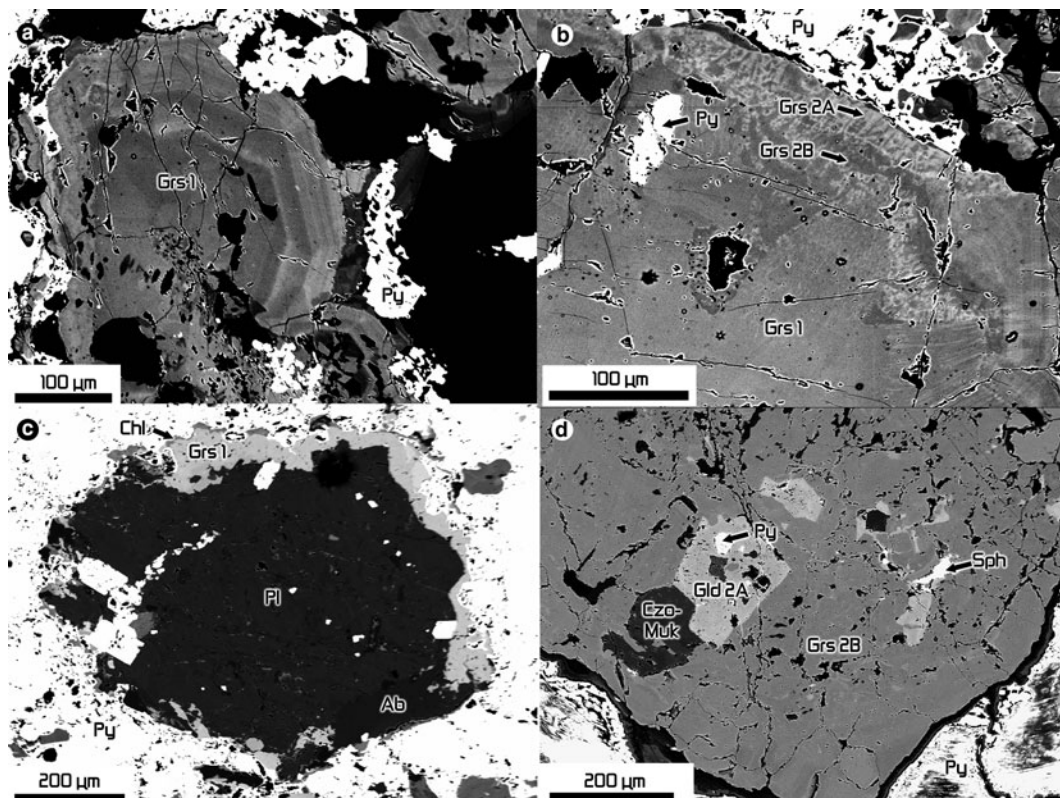


FIG. 2. Back-scattered electron images of garnets and associated minerals: (a) primary V-Cr and Mn-rich grossular (Grs 1) forming subhedral crystals with oscillatory zoning; (b) detail of homogeneous primary grossular crystal (Grs 1) with irregular alteration domains along the rim consisting of secondary grossular (pale grey Grs 2A and darker grey Grs 2B); (c) Grs 1 grossular on the rim of plagioclase (Pl) grain with albite (Ab), chlorite (Chl) and pyrite (Py); (d) large crystal of secondary grossular (Grs 2B) with irregular patchy domains of goldmanite (Gld 2A) in association with clinzoisite-mukhinitite (Czo-Muk), sphalerite (Sph) and pyrite (Py).

Whereas garnet titanium contents are also generally low, the Grs 1 grossular has somewhat higher Ti concentrations (0.03–0.06 apfu) compared to secondary garnet types (<0.04 apfu Ti) (Table 1, Fig. 3c). Vanadium correlates positively with Cr, with the garnet V:Cr atomic ratio usually between 1:1 and 2:1 (Fig. 3d). Dominant garnet substitutions include CaMn_{-1} at the X site and (V, Cr) Al_{-1} at the Y site, resulting in coupled $\text{Ca(V,Cr)Mn}_{-1}\text{Al}_{-1}$ mechanism (Fig. 3e–h).

Garnet trace-element contents were determined by LA-ICP-MS (Table 2). Yttrium is the most abundant trace element with contents up to ~3600 ppm, and heavy REEs (HREE) are also relatively enriched, with Dy, Er and Yb varying between 30 and 370 ppm. The dominant role of HREE in garnets is documented in the chondrite-

normalized REE diagram (Fig. 4a). The contents of other trace elements, including Ge, Ga, Zr, Zn and Sn, do not exceed 100 ppm.

Epidote-supergroup minerals

The Epidote-supergroup minerals occur as abundant anhedral crystals 0.1 to 2 mm in size. Although these single crystals are commonly isolated and surrounded by pyrite (Py) (Fig. 5a), in some places they occur in close association with other minerals; mainly with apatite (Ap), Ba-rich feldspar (Ba-Fs) and plagioclase (Pl) with variable anorthite content, and these constitute the primary mineral association (Fig. 5b,c). However, they are commonly overgrown by chlorite (Chl), quartz

TABLE 1. Representative compositions of garnet-supergroup minerals from Čierna Lehota.

Sample #	CL-1.4	CL-1.5	CL-1.32	CL-4.26	CL-4.28	CL-1.1	CL-4.31	CL-4.32	CL-1.2	CL-1.3	CL-1.39	CL-1.33	CL-1.42	CL-4.27
Garnet type	Grs 1	Grs 1	Grs 1	Gld 2A	Gld 2A	Gld 2B	Gld 2B	Gld 2B	Grs 2A	Grs 2A	Grs 2A	Grs 2B	Grs 2B	Sps 2
Wt. %														
SiO ₂	36.44	36.69	36.68	35.34	35.44	36.12	35.50	36.28	36.73	36.81	37.48	38.02	38.26	37.19
TiO ₂	0.85	0.58	0.94	0.14	0.26	0.12	0.24	0.26	0.34	0.46	0.28	0.26	0.36	0.40
Al ₂ O ₃	12.69	14.69	11.53	3.87	4.28	6.67	4.76	7.20	8.07	10.43	9.98	21.13	21.00	20.32
V ₂ O ₃	7.12	5.29	8.49	17.39	16.78	11.96	13.21	12.47	10.56	8.63	8.94	0.23	0.21	0.41
Cr ₂ O ₃	4.30	3.48	4.50	8.47	8.41	8.92	10.65	7.93	7.52	6.36	6.50	0.33	0.05	0.64
Fe ₂ O ₃ *	0.22	0.53	–	0.53	0.57	–	0.87	0.26	–	–	0.20	–	–	1.88
FeO*	1.66	1.80	1.70	–	–	1.55	–	1.01	1.09	1.67	0.82	4.72	3.93	1.90
MnO	14.37	17.67	13.63	3.66	3.11	9.31	4.89	5.77	7.95	10.30	7.16	17.10	18.19	21.23
NiO	–	0.02	0.02	0.01	–	–	0.03	0.02	–	0.05	0.01	–	–	–
ZnO	–	–	0.02	0.02	0.02	–	–	0.03	–	–	0.06	0.05	0.03	0.01
MgO	0.25	0.59	0.60	0.12	0.14	–	0.14	0.26	–	0.11	0.84	0.46	0.49	0.57
CaO	21.58	18.41	21.38	30.19	30.69	24.92	29.23	28.30	27.21	24.64	27.58	17.42	17.20	15.92
Na ₂ O	–	–	0.07	–	–	–	–	–	0.01	0.04	0.02	0.06	0.04	–
Total	99.48	99.75	99.56	99.75	99.72	99.57	99.53	99.78	99.47	99.50	99.88	99.78	99.77	100.47
Atoms per formula unit on the basis of 8 cations														
Si	2.948	2.950	2.985	2.924	2.924	2.979	2.938	2.965	2.994	2.986	3.011	2.996	3.017	2.941
Al Z	0.052	0.050	0.015	0.076	0.076	0.021	0.062	0.035	0.006	0.014	0.000	0.004	0.000	0.059
Sum Z	3.000	3.000	3.000	3.000	3.000	3.000	3.000	3.000	3.000	3.000	3.011	3.000	3.017	3.000
Ti	0.052	0.035	0.057	0.009	0.016	0.008	0.015	0.016	0.021	0.028	0.017	0.015	0.022	0.024
Al Y	1.158	1.341	1.092	0.301	0.340	0.627	0.403	0.658	0.770	0.983	0.945	1.960	1.952	1.834
V	0.462	0.341	0.554	1.154	1.110	0.791	0.877	0.817	0.690	0.562	0.576	0.015	0.014	0.026
Cr	0.275	0.221	0.289	0.554	0.549	0.582	0.697	0.513	0.485	0.408	0.413	0.020	0.003	0.040
Fe ³⁺	0.013	0.032	0.000	0.033	0.035	–	0.054	0.016	–	–	0.012	–	–	0.113
Sum Y	1.960	1.970	1.992	2.050	2.050	2.008	2.045	2.019	1.965	1.981	1.963	2.010	1.990	2.036
Fe ²⁺	0.112	0.121	0.116	0.000	–	0.107	0.000	0.069	0.074	0.113	0.055	0.311	0.259	0.126
Mn	0.985	1.203	0.940	0.256	0.217	0.650	0.343	0.399	0.549	0.707	0.487	1.142	1.215	1.422
Ni	–	0.002	0.001	0.001	–	–	0.002	0.001	–	0.003	0.001	–	–	–
Zn	–	–	0.001	0.001	0.001	–	–	0.002	–	–	0.003	0.003	0.002	0.001
Mg	0.030	0.071	0.072	0.015	0.018	–	0.018	0.031	–	0.013	0.101	0.054	0.058	0.067
Ca	1.871	1.586	1.865	2.676	2.713	2.203	2.592	2.478	2.377	2.142	2.375	1.471	1.454	1.349
Na	–	–	0.012	0.000	–	–	–	–	0.001	0.007	0.003	0.010	0.006	–
Sum X	2.998	2.982	3.007	2.949	2.950	2.960	2.955	2.981	3.001	2.985	3.025	2.990	2.992	2.964

*FeO and Fe₂O₃ were calculated from charge-balanced formula.
 ‘–’ = not detected

(Qz) and almost pure albite (Ab) (Fig. 5a), while pyrite and other rarer sulfides including chalcopyrite (Ccp) and sphalerite (Sph) commonly occur along fissures in epidote-supergroup minerals.

The epidote-supergroup minerals from Čierna Lehota have variable chemical zoning and evolution. Moreover, extensive compositional variation at the *M* sites, especially at the *M1* and *M3* sites, makes unambiguous site assignment difficult. Therefore, the occupancy of these sites is not divided in the formulae used here.

Some crystals have a complete zoning sequence with the oldest allanite-(La) and REE- and Mg-rich mukhinite containing a large proportion of dissakisite-(La) component (Aln-Muk) rimmed by V- and Cr-rich clinzoisite to mukhinite parts

attaining compositions close to allanite-(La) composition (Czo-Muk) and V- and Cr-poor clinzoisite (Czo) (Figs 5 and 6). However, the majority of the epidote-supergroup minerals do not have completely evolved zones, with only Czo-Muk in the core and Czo on the rim (Fig. 5a). Chromium and V are correlated positively, but this correlation is relatively poor with considerable scatter in the data suggesting irregular distribution of Cr in the most Cr and V enriched zones (Fig. 6b).

The transition between zones is also irregular; where Czo-Muk penetrates and resorbs Aln-Muk (Fig. 5d,e). Although the border between Czo-Muk and Czo is irregular, it is sharper, and there is textural difference between zones; for example, Aln-Muk zone has a system of almost parallel

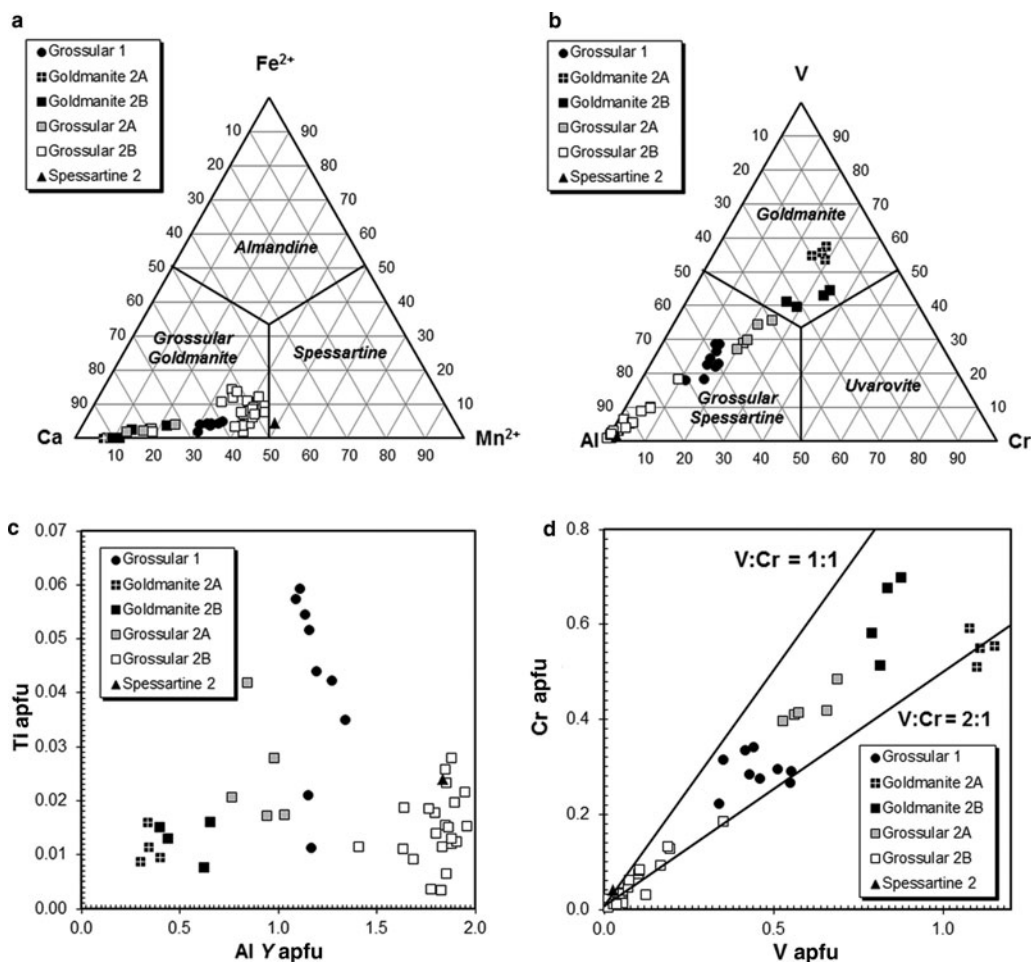


FIG. 3. Classification and substitution diagrams for garnet-supergroup minerals.

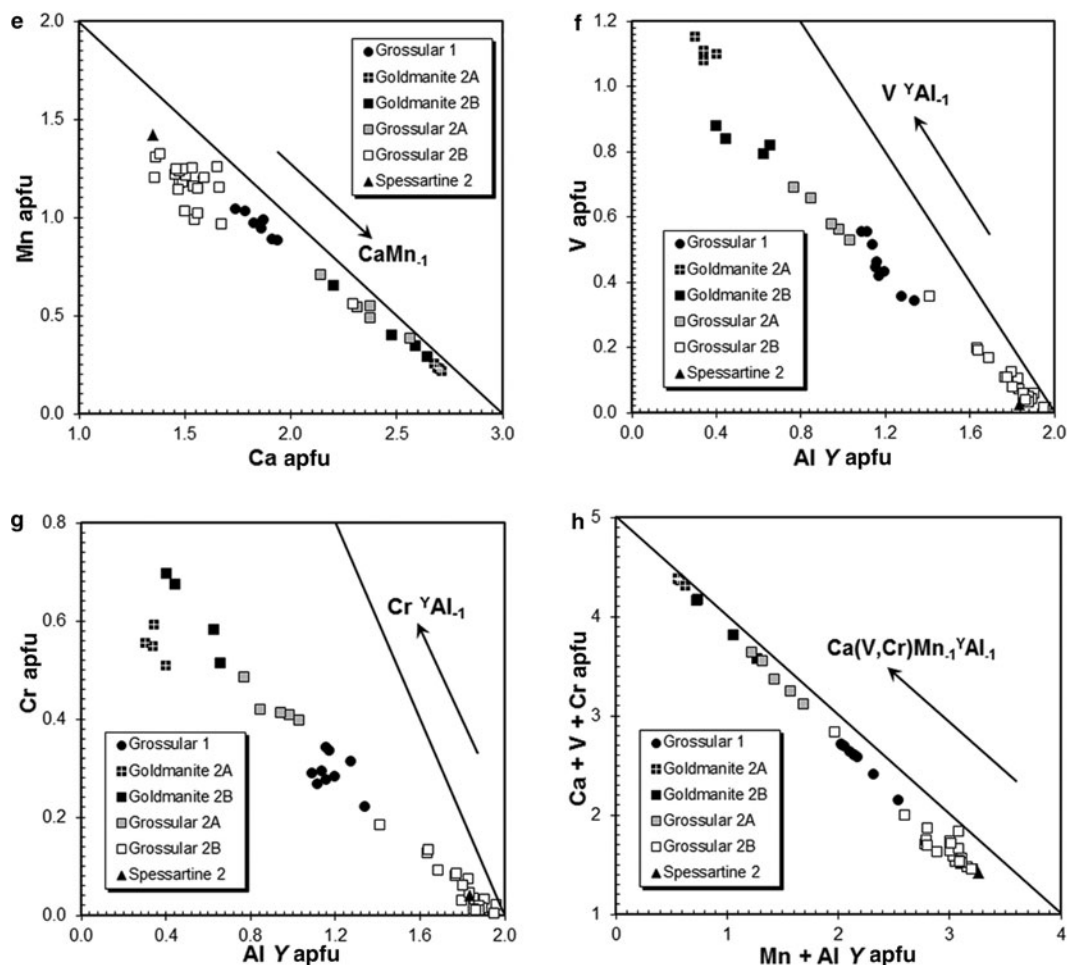


FIG. 3. (Continued).

cracks which do not extend to other zones (Fig. 5d, f). The Aln-Muk zone has weak compositional zoning with irregularly distributed zones with mukhinite-(La) composition (darker grey in back-scattered electron image) in major allanite-(La) (Fig. 5f). In contrast, the Czo-Muk zone displays very strong irregular zoning based on variations in V, Cr, Fe, Al and REE (Fig. 5e). Finally, the Czo zone has weak zoning induced by the decrease in V and Cr from the border between Czo-Muk and Czo towards the outer rim (Fig. 5a).

Allanite-(La) and Mg- and REE-rich mukhinite is the most enriched in La (up to 0.407 apfu), the La/Ce ratio is 2.05–2.62, the La/Nd ratio is 1.47–2.10, and even the content of Nd (0.076–0.204 apfu) is higher than Ce (0.036–0.158 apfu)

and Nd/Ce is 1.25–2.12, resulting in a negative Ce anomaly (Table 3). Ferrous iron usually dominates over Mg in most of the Aln-Muk zone with $Fe^{2+}/(Fe^{2+}+Mg)$ between 0.79 and 0.91; Mg is the dominant divalent cation at the *M3* site only in irregular zones and veins of mukhinite, with $Fe^{2+}/(Fe^{2+}+Mg)$ between 0.11 and 0.20 (Table 3). Both allanite-(La) and Mg- and REE-rich mukhinite are also rich in V (0.14–0.36 apfu) and Cr (0.02–0.11 apfu). The structural formulae of allanite-(La) suggest that some V and/or Cr is located at the *M1* site; at least in compositions with *M*Al content lower than 2 apfu (Fig. 6b). However, without crystallographic data it is impossible to determine the actual extent of the Al-Cr and/or Al-V disorder. Allanite-(La) is also enriched in

TABLE 2. Contents of trace elements (in ppm) in garnet- and epidote-supergrout minerals. Analysed with LA-ICP-MS.

	⁴⁵ Sc	⁴⁷ Ti	⁵⁹ Co	⁶⁰ Ni	⁶⁶ Zn	⁷¹ Ga	⁷⁴ Ge	⁸⁸ Sr	⁸⁹ Y	⁹⁰ Zr	⁹³ Nb	¹¹⁸ Sn	¹³³ Cs	¹³⁷ Ba
Grt	10	460	b.d.l.	b.d.l.	30	30	20	b.d.l.	388	10	b.d.l.	35	b.d.l.	0.1
Grt	63	4313	0.3	b.d.l.	16	25	60	0.2	2683	8	2.6	38	b.d.l.	0.2
Grt	45	2044	b.d.l.	3.9	35	27	81	1.2	3584	26	0.2	39	0.1	1.5
Czo	274	311	b.d.l.	b.d.l.	80	229	43	1283	6000	11	b.d.l.	92	0.2	32
d.l.	5	4	0.3	2	2	0.4	0.1	0.1	0.1	0.1	0.1	5	0.1	0.1
	¹³⁹ La	¹⁴⁰ Ce	¹⁴¹ Pr	¹⁴⁶ Nd	¹⁴⁷ Sm	¹⁵³ Eu	¹⁵⁷ Gd	¹⁵⁹ Tb	¹⁶³ Dy	¹⁶⁵ Ho	¹⁶⁶ Er	¹⁶⁹ Tm	¹⁷² Yb	¹⁷⁵ Lu
Grt	b.d.l.	b.d.l.	b.d.l.	0.6	2.7	2.6	13	3	29	9	35	5	37	6
Grt	b.d.l.	b.d.l.	b.d.l.	0.3	2.3	1.2	28	14	177	65	231	37	250	37
Grt	0.3	0.2	0.1	1.4	2.1	2.7	26	13	204	83	321	53	371	53
Czo	13,699	4878	2423	10,419	1600	295	1327	157	902	174	387	41	206	27
d.l.	0.1	0.1	0.1	0.3	0.1	0.1	0.1	0.1	0.1	0.1	0.1	0.1	0.1	0.1
	¹⁷⁸ Hf	¹⁸¹ Ta	²⁰⁶ Pb	²⁰⁷ Pb	²⁰⁸ Pb	²³² Th	²³⁵ U	²³⁸ U						
Grt	b.d.l.	0.2												
Grt	0.4	0.1	0.7	b.d.l.	b.d.l.	b.d.l.	b.d.l.	2.8						
Grt	0.4	b.d.l.	0.5	b.d.l.	0.1	b.d.l.	b.d.l.	2.9						
Czo	0.5	0.1	145	12	10	182	2412	755						
d.l.	0.1	0.1	0.2	0.3	0.1	0.1	19	0.1						

d.l.—detection limit; b.d.l.—below detection limit

Mn²⁺ (0.09–0.23 apfu) and Mg- and REE-rich mukhinite is slightly depleted, with Mn only up to 0.05 apfu (Table 3). Stoichiometry of the analyses requires that part of the Mn is located at the A1 site. Interestingly, allanite-(La) is enriched in Na (0.05–0.10 apfu), while it is only slightly above the detection limit (up to 0.003 apfu) in mukhinite and in other zones apart from the REE-rich Czo-Muk.

The Czo-Muk zone displays large compositional variability. When the Aln-Muk core is present, the composition of epidote-supergrout minerals in the Czo-Muk zone is REE-enriched with up to 0.40 apfu (Table 3). Interestingly, the proportions of individual REE differ from the proportions in Aln-Muk in that the La/Ce ratio is 2.05–2.13 and the Nd/Ce ratio is 2.08–2.13. Furthermore, the La/Nd ratio in Czo-Muk is 0.96–1.03 which indicates that Nd is the dominant REE in part of this zone. In contrast, the REE content is lower in crystals lacking the Aln-Muk core; not exceeding 0.36 apfu REE and usually below 0.1 apfu. However, the REE-depleted parts of crystals are enriched in V (up to 0.45 apfu) and Cr (up to 0.29 apfu) attaining mukhinite composition (Table 3). The REE-rich and REE-depleted parts of Czo-Muk zone are well separated, but irregular in spatial distribution.

Aluminium is the most abundant octahedral cation, fully occupying the M1 and M2 sites (except for possible disorder with V and Cr) and it varies between 0.22 and 0.71 apfu at the M3 site. After V, Fe²⁺ is the third most abundant octahedral cation with up to 0.38 apfu. The Mg content also increases in some places up to 0.26 apfu. Both Fe²⁺ and Mg correlate well positively with REE content. Moreover, part of the Fe (up to 0.20 apfu) is calculated as ferric. Although Mn is lower with no more than 0.06 apfu compared to its concentration in the Aln-Muk zone, it can increase up to 0.12 apfu, but only in parts attaining allanite composition.

The most external zone has the following composition; REE- (up to 0.02 apfu), V- (up to 0.07 apfu) and Cr-poor clinozoisite (up to 0.04 apfu). The content of divalent octahedral cations such as Fe²⁺ (up to 0.03 apfu), Mg (up to 0.01 apfu) and Mn (up to 0.04 apfu) is also very low, which makes Fe³⁺ (0.01–0.20 apfu) the dominant substituent of Al in octahedral sites. The A sites are dominated by Ca (1.96–1.99 apfu).

The composition of epidote-supergrout minerals is influenced by several sets of coupled substitutions. Heterovalent substitutions expressed as

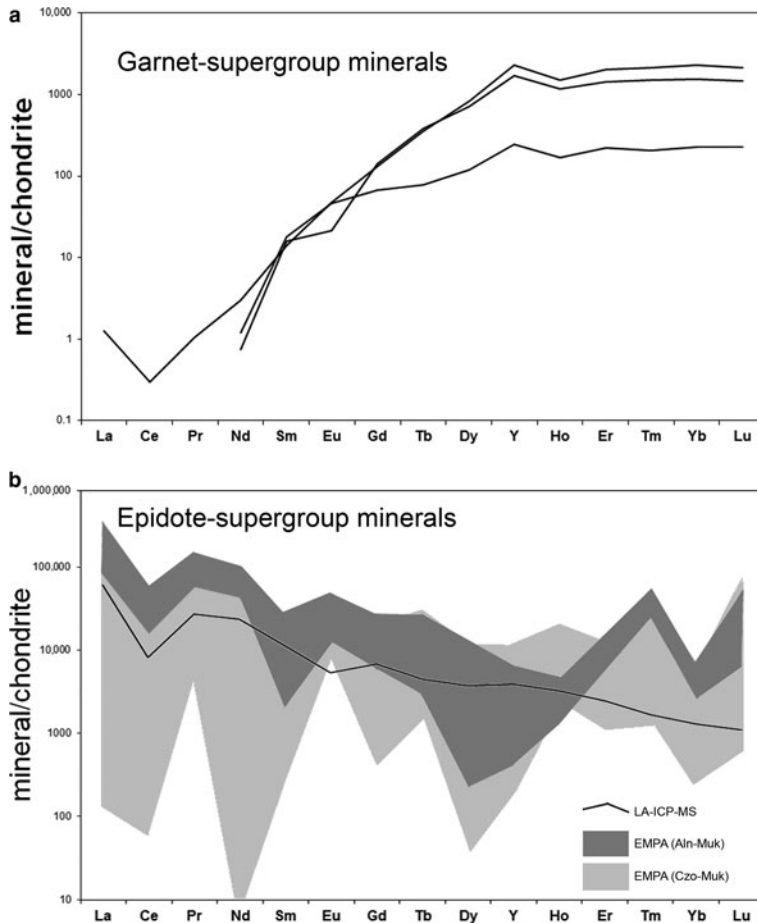


FIG. 4. Average chondrite-normalized *REE* distribution patterns of (a) garnet- and (b) epidote-supergroup minerals from Čierna Lehota based on LA-ICP-MS (a, b) and EMPA (b) data. Chondrite values from Anders and Grevesse (1989).

$A2^{3+}M^{2+}(A2^{2+}M^{3+})_{-1}$ result in a compositional trend from clinzoisite to allanite-(La) and dissakisite-(La) (Fig. 7a). The resulting trend (Fig. 7b) is the sum of several substitutions including $REEFe^{2+}(CaAl)_{-1}$, $REEMg(CaAl)_{-1}$, $REEMn^{2+}(CaAl)_{-1}$ and $REEFe^{2+}(CaFe^{3+})_{-1}$. Deviations in the trend from an ideal correlation are due to homovalent substitutions at the *M* sites such as $VA1_{-1}$ and $CrAl_{-1}$ (Fig. 7c). Homovalent substitutions at the *A2* site are limited only to variations in *REE*, and the increase in Na in allanite-(La) can be attributed to the coupled heterovalent substitution $^{A1}NaR^{3+}(^{A1}CaR^{2+})$.

Epidote-supergroup minerals are enriched in U, Sr, Sc, Ga and Pb, whereas other elements including Sn, Ge and Ba are <100 pm in

concentrations. Enrichment in *REE* is also documented in LA-ICP-MS analysis (Table 2). Chondrite-normalized distribution patterns from EMPA and LA-ICP-MS are similar and show marked negative Ce anomalies (Fig. 4b). Whereas patterns from EMPA analyses have positive Eu anomalies, the LA-ICP-MS Eu anomaly is also negative.

Discussion and conclusions

Crystal chemistry of garnet-supergroup minerals

All five compositional types of garnets from Čierna Lehota have notable enrichment in V, Cr and partly

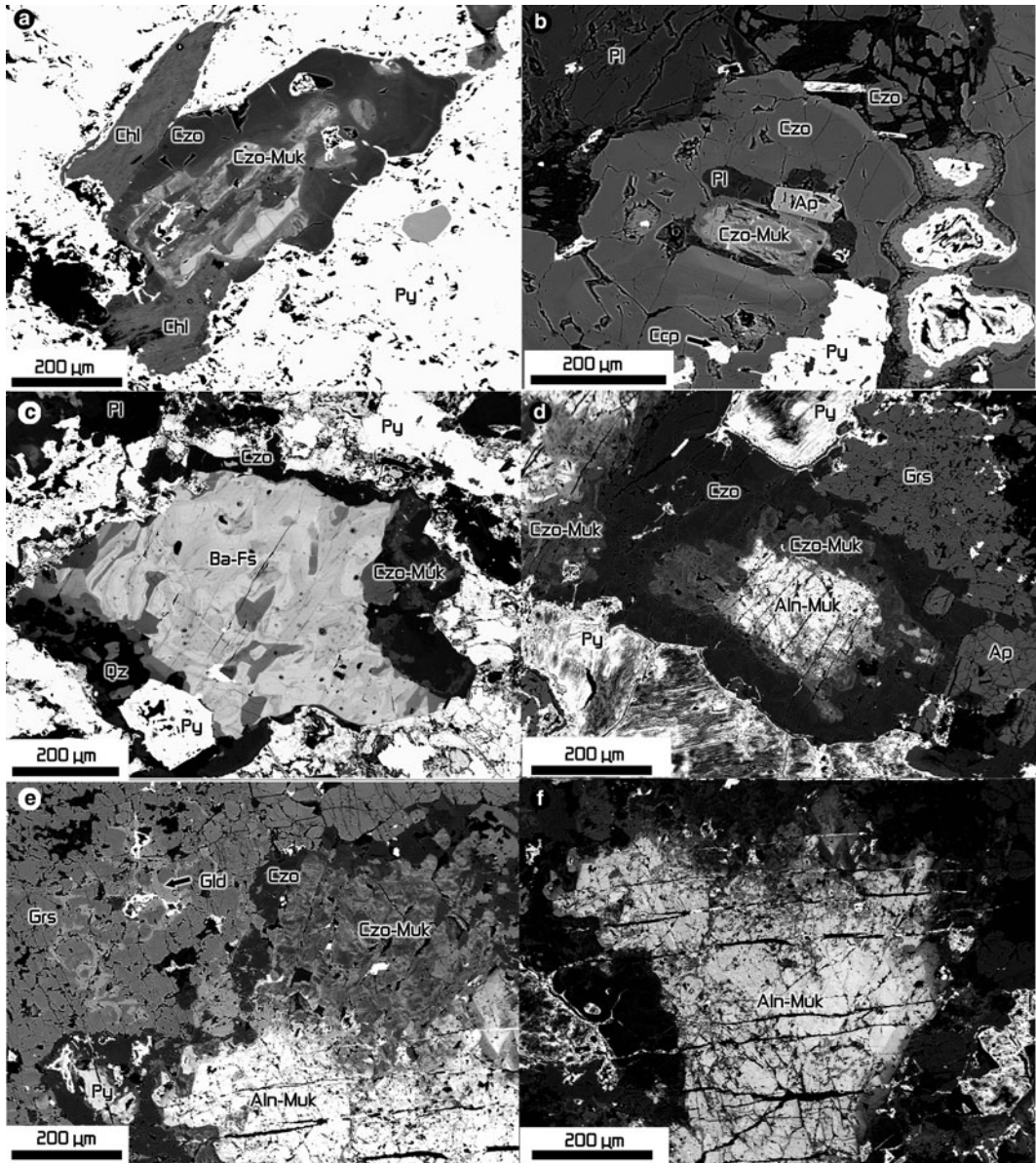


FIG. 5. Back-scattered electron images of epidote-super group and associated minerals: (a) Isolated grain of epidote-super group mineral with distinct clinozoisite-mukhinite (Czo-Muk) and clinozoisite (Czo) zones overgrown by chlorite (Chl) and pyrite (Py); (b) Czo-Muk in association with plagioclase (Pl) and apatite (Ap) overgrown by Czo with chalcocopyrite (Ccp) and Py; (c) Rim of Czo-Muk, Czo and quartz (Qz) around barium-rich feldspar (Ba-Fs); (d) grain of epidote-super group mineral with allanite-mukhinite (Aln-Muk) core and Czo-Muk and Czo zones associated with grossular (Grs) and Ap; (e) crystals of epidote- (Aln-Muk, Czo-Muk and Czo zones) and garnet- (Gld and Grs) group mineral in contact. Czo-Muk zone displays patchy zoning; (f) Aln-Muk zone of the crystal shown in (e) is cut by a system of parallel cracks that are spatially limited to this zone.

TABLE 3. Representative compositions of epidote-supergroup minerals from Čierna Lehota (wt.%) and converted to apfu on the basis of 8 cations according to the procedure in Armbruster *et al.* (2006).

Sample #	CL-4	CL-4	CL-4	CL-4	CL-4	CL-4	CL-4	CL-4
Zone	Aln-Muk	Aln-Muk	Aln-Muk	Czo-Muk	Czo-Muk	Czo-Muk	Czo	Czo
Mineral	Aln-(La)	Aln-(La)	Muk	Muk	Czo	Czo	Czo	Czo
Wt.%								
SiO ₂	31.62	32.90	34.83	37.34	38.24	36.85	38.40	38.93
TiO ₂	0.20	0.07	0.09	0.05	0.17	0.07	0.09	0.14
Al ₂ O ₃	16.26	19.13	21.67	23.71	28.99	25.06	29.31	29.91
V ₂ O ₃	4.59	4.51	3.74	6.97	1.88	2.47	1.85	0.40
Cr ₂ O ₃	0.34	0.33	1.57	4.54	1.22	0.89	0.57	0.13
Fe ₂ O ₃ *	–	0.38	–	0.90	2.28	–	2.57	3.45
FeO*	8.10	5.56	1.08	–	–	0.79	–	0.24
MnO	2.25	3.00	0.71	–	0.60	0.38	0.56	0.61
MgO	0.43	0.62	2.44	–	–	1.94	–	0.06
NiO	0.04	0.01	0.01	–	–	0.03	0.02	–
BaO	0.05	0.08	0.05	0.02	0.01	0.02	0.01	–
SrO	0.08	0.24	0.06	0.12	0.14	0.10	0.10	–
CaO	10.01	10.77	16.66	23.09	23.28	19.26	23.90	23.62
Na ₂ O	0.28	0.55	0.02	0.01	0.02	0.01	0.03	–
K ₂ O	–	–	–	–	–	–	–	–
La ₂ O ₃	11.56	8.53	5.72	0.02	–	3.41	0.03	–
Ce ₂ O ₃	4.43	3.30	2.43	0.01	0.04	1.84	–	–
Pr ₂ O ₃	1.81	1.47	1.12	0.17	0.06	0.79	0.10	–
Nd ₂ O ₃	5.72	5.47	3.98	0.02	–	2.70	–	–
Sm ₂ O ₃	–	–	0.04	–	–	0.33	–	–
Eu ₂ O ₃	0.31	0.32	0.16	0.09	0.17	0.09	0.10	–
Gd ₂ O ₃	0.15	0.37	0.28	–	0.06	0.35	0.01	–
Tb ₂ O ₃	0.04	0.03	0.03	–	0.04	0.07	0.04	–
Dy ₂ O ₃	–	0.12	0.10	0.02	0.10	0.18	–	–
Ho ₂ O ₃	–	–	–	–	–	0.06	–	–
Er ₂ O ₃	0.22	0.18	0.20	0.23	0.22	0.14	0.11	–
Tm ₂ O ₃	0.08	0.16	0.12	0.01	0.06	0.09	–	–
Yb ₂ O ₃	0.06	0.13	0.09	0.07	0.06	0.13	0.08	–
Lu ₂ O ₃	0.08	0.09	0.12	–	0.06	0.01	0.04	–
Y ₂ O ₃	0.14	0.44	0.60	0.26	0.79	0.39	0.05	–
UO ₂	0.05	0.07	0.01	0.05	–	0.09	–	–
ThO ₂	0.06	0.10	0.05	–	–	0.05	0.01	–

F	–	–	–	–	–	–	–	–	–
Cl	0.02	0.01	0.01	–	0.01	0.03	–	–	0.01
H ₂ O [†]	1.58	1.65	1.75	1.88	1.93	1.83	1.94	–	1.94
Total	100.54	100.59	99.75	99.55	100.41	100.42	99.92	–	99.44
O = F	0.00	0.00	0.00	0.00	0.00	0.00	0.00	–	0.00
O = Cl	–0.01	–0.01	–0.01	0.00	0.00	–0.01	0.00	–	0.00
Total	100.53	100.59	99.74	99.55	100.41	100.41	99.92	–	99.43
Atoms per formula unit on the basis of 8 cations									
Si ⁴⁺	2.990	2.986	2.986	2.976	2.970	3.018	2.973	–	3.011
Al ³⁺	0.010	0.014	0.014	0.024	0.030	0.000	0.027	–	0.000
<i>T</i>	3.000	3.000	3.000	3.000	3.000	3.018	3.000	–	3.011
Al ³⁺	1.000	1.000	1.000	1.000	1.000	1.000	1.000	–	1.000
<i>M2</i>	1.000	1.000	1.000	1.000	1.000	1.000	1.000	–	1.000
Ti ⁴⁺	0.014	0.004	0.006	0.003	0.010	0.004	0.005	–	0.008
Al ³⁺	0.803	1.032	1.176	1.204	1.623	1.419	1.649	–	1.727
Cr ³⁺	0.025	0.024	0.107	0.286	0.075	0.058	0.035	–	0.008
V ³⁺	0.348	0.328	0.257	0.446	0.117	0.162	0.115	–	0.025
Fe ³⁺	–	0.026	–	0.054	0.134	–	0.150	–	0.201
Fe ²⁺	0.641	0.422	0.077	–	–	0.054	–	–	0.015
Mn ²⁺	0.106	0.079	0.000	–	0.000	0.000	–	–	0.009
Mg ²⁺	0.060	0.085	0.312	–	–	0.237	–	–	0.006
Ni ²⁺	0.003	0.001	0.001	–	–	0.002	0.001	–	–
<i>M1 + M3</i>	2.000	2.000	1.935	1.992	1.959	1.936	1.954	–	2.000
Ca ²⁺	0.948	0.903	0.998	0.999	0.997	0.998	0.995	–	1.000
Na ⁺	0.052	0.097	0.002	0.001	0.003	0.002	0.005	–	–
Mn ²⁺	0.074	0.151	0.052	–	0.039	0.026	0.037	–	0.031
Al	1.000	1.000	1.000	1.000	1.000	1.000	1.000	–	1.000
Ca ²⁺	0.066	0.144	0.533	0.973	0.940	0.692	0.988	–	0.958
U ⁴⁺	0.001	0.001	0.000	0.001	–	0.002	–	–	–
Th ⁴⁺	0.001	0.002	0.001	–	–	0.001	–	–	–
Y ³⁺	0.007	0.021	0.027	0.011	0.032	0.017	0.002	–	–
La ³⁺	0.403	0.286	0.181	0.001	–	0.103	0.001	–	–
Ce ³⁺	0.153	0.110	0.076	0.000	0.001	0.055	–	–	–
Pr ³⁺	0.062	0.049	0.035	0.005	0.002	0.023	0.003	–	–
Nd ³⁺	0.193	0.177	0.122	0.001	–	0.079	–	–	–
Sm ³⁺	–	–	0.001	–	–	0.009	–	–	–
Eu ³⁺	0.010	0.010	0.005	0.002	0.004	0.003	0.003	–	–
Gd ³⁺	0.005	0.011	0.008	–	0.002	0.009	–	–	–
Tb ³⁺	0.001	0.001	0.001	–	0.001	0.002	0.001	–	–

(continued)

TABLE 3. (contd.)

Sample #	CL-4	CL-4	CL-4	CL-4	CL-4	CL-4	CL-4	CL-16
Zone	Aln-Muk	Aln-Muk	Aln-Muk	Czo-Muk	Czo-Muk	Czo-Muk	Czo	Czo
Mineral	Aln-(La)	Aln-(La)	Muk	Muk	Czo	Czo	Czo	Czo
Dy ³⁺	–	0.003	0.003	–	0.003	0.005	–	–
Ho ³⁺	–	–	–	–	–	0.002	–	–
Er ³⁺	0.006	0.005	0.005	0.006	0.005	0.004	0.003	–
Tm ³⁺	0.002	0.005	0.003	0.000	0.001	0.002	–	–
Yb ³⁺	0.002	0.004	0.002	0.002	0.001	0.003	0.002	–
Lu ³⁺	0.002	0.003	0.003	–	0.001	0.000	0.001	–
Ba ²⁺	0.002	0.003	0.002	–	–	0.001	–	–
Sr ²⁺	0.004	0.013	0.003	0.006	0.006	0.005	0.005	–
K ⁺	–	–	–	–	–	–	–	–
A2	0.922	0.847	1.012	1.008	1.001	1.016	1.008	0.958
F [–]	–	–	–	–	–	–	–	–
Cl [–]	0.004	0.002	0.002	–	0.001	0.004	–	0.001
OH [–]	1.000	1.000	1.000	1.000	1.000	1.000	1.000	1.000

*Fe₂O₃ and FeO calculated from charge-balanced formula; †H₂O calculated assuming OH = 1 pfu

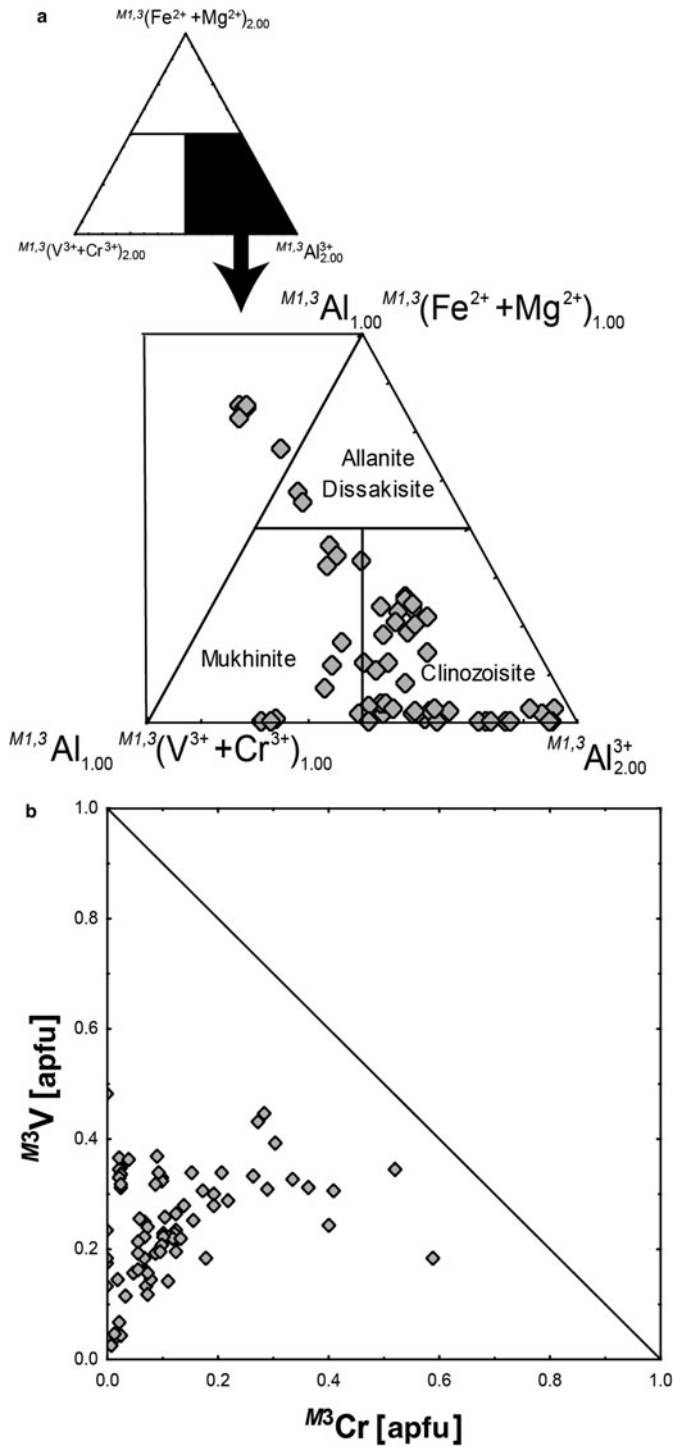


FIG. 6. Diagrams for epidote-supergroup minerals: (a) classification diagram involving dominant $M1$ - and $M3$ -site cations; (b) plot of M^3V (apfu) vs. M^3Cr (apfu).

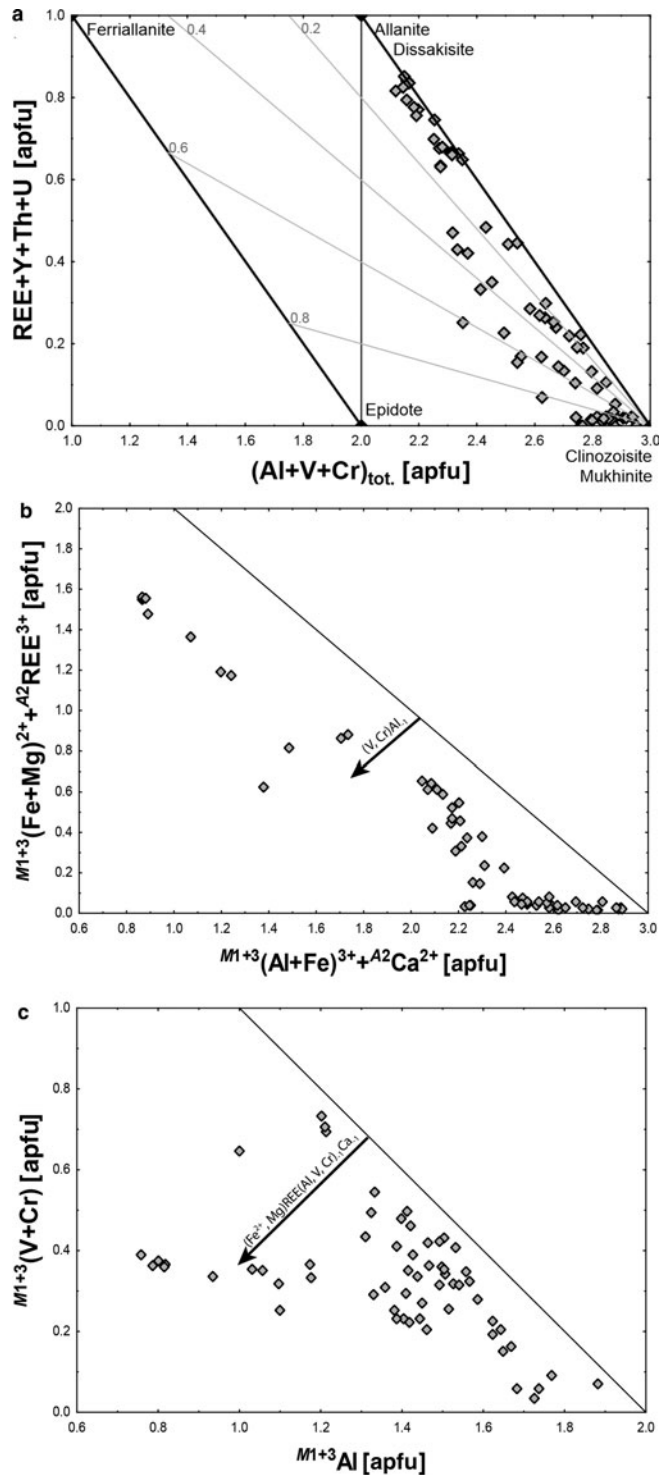


FIG. 7. Substitution diagrams for epidote-supergroup minerals. Fig. 7a modified after Petřík *et al.* (1995)

also Mn. The garnet minerals primarily belong to a complex goldmanite–uvarovite–grossular–momoiite–spessartine solid solution. On the basis of textural relationships, the primary metamorphic grossular (Grs 1) contains elevated V, Cr and Mn concentrations (0.34–0.55 apfu V, 0.22–0.34 apfu Cr and 0.88–1.20 apfu Mn). This grossular is interpreted as a precursor to secondary goldmanite and grossular–spessartine solid solution (Gld 2A, Gld 2B, Grs 2A, Grs 2B–Sps 2, Fig. 3), which form irregular domains with convolute, vermicular, lamellar and mosaic textures, locally riddled with tiny voids. The secondary garnet has partly replaced the primary Grs 1 grossular (Fig. 2*b,d*). These textures and microporosity indicate later-stage metasomatic alteration of Grs 1 by a fluid-driven dissolution–reprecipitation process (Putnis 2002, 2009). Consequently, these two processes of primary metamorphic crystallization and secondary metasomatic overprint caused the unusual compositional variability and complex V–Cr- and Mn-rich compositions of the Čierna Lehota garnets.

The vanadium-rich garnets (V-rich grossular to goldmanite), commonly in association with other V-rich silicate phases (mainly minerals of the epidote supergroup, mica supergroup, pyroxene group, amphibole supergroup and titanite) have been reported from numerous metamorphic rocks enriched in organic carbon and vanadium and V-rich silicate minerals (Moench and Meyrowitz, 1964; Shepel and Karpenko, 1969; Karev, 1974; Litochleb *et al.*, 1985, 1997; Benkerrou and Fonteilles, 1989; Pan and Fleet, 1991; Jeong and Kim, 1999). However, these V-rich garnets are usually poor in Cr and Mn. Rarely, V-rich grossular–goldmanite also have distinct Cr enrichment (Filippovskaya *et al.*, 1972; Uher *et al.*, 1994, 2008; Canet *et al.*, 2003; Makrygina *et al.*, 2004). Moreover, a distinctive compositional group comprises Mn-rich vanadian garnets, including the Mn, V-rich grossular–V-rich spessartine–momoiite ($\text{Mn}_3\text{V}_2\text{Si}_3\text{O}_{12}$)–Mn-rich goldmanite solid solution from several metamorphic Mn deposits in Japan (Momoi, 1964; Kato *et al.*, 1994; Tanaka *et al.*, 2010; Matsubara *et al.*, 2010) and also in the Domoradice graphite deposit in the Czech Republic (Černý *et al.*, 1995).

Crystal chemistry of epidote-supergroup minerals

The crystal chemistry of V-, Cr- and REE-rich epidote-supergroup minerals from Čierna Lehota is

influenced by a variety of substitutions. For example, Cr and V are incorporated in both the REE-free (e.g. Shepel and Karpenko, 1969; Treolar, 1987*a*) and REE-rich epidote-supergroup minerals members. (Ovchinnikov and Tzimbalenko, 1948; Rao and Babu, 1978; Treolar and Chamley, 1987; Yang and Enami, 2003; Bačík and Uher, 2010); In Čierna Lehota, these elements are present in both REE-rich and REE-free compositions. Vanadium content is the highest in the Czo–Muk zone where it attains the mukhinite composition with up to 0.45 V apfu (7.0 wt.% V_2O_3).

Both Cr and V occupy the octahedral *M* sites by homovalent substitutions with Al. Vanadium usually enters the structure of epidote-supergroup minerals as V^{3+} because only an extremely oxidizing environment allows V^{5+} stabilization in epidote-supergroup minerals (Gieré and Sorensen, 2004). The behaviour of Cr in the epidote-supergroup minerals structure is unclear due to the possible Al–Cr disorder between the *M1* and *M3* sites (Armbruster *et al.*, 2006; Nagashima *et al.*, 2007). It is even more enigmatic in the light of previous research on Cr-rich clinozoisite from Finland and Japan with presumed exsolution of a V- and Cr-bearing phase from a clinozoisite structure (Nagashima *et al.*, 2011). If a V- and Cr-bearing epidote-supergroup mineral phase showing Al–Cr disorder, such as the amorphous phase reported by Nagashima *et al.* (2011), were present in epidote-supergroup minerals from Čierna Lehota, we found no evidence for it in the available analytical data. Indeed, we are not aware of any evidence reported for Al– V^{3+} disorder at the *M1* and *M3* sites, although potentially such disorder is possible in epidote-supergroup minerals. However, the abundance of octahedral cations other than Al, including Fe^{2+} , Mn^{2+} and V in some compositions of allanite-(La) from Čierna Lehota, suggests that V could be distributed in both *M1* and *M3* sites. This presumption is based on the geometry of the octahedral sites, where the *M3* site is larger and more distorted than both *M1* and *M2* sites (Dollase, 1968) and also on REE occupancy at the *A2* site, which requires divalent cations in the *M3* octahedra (Nagashima *et al.*, 2007). Vanadium, which is smaller (0.64 Å) than Fe^{2+} (0.78 Å) and Mn^{2+} (0.83 Å), is the most probable substituent for Al^{3+} (0.535 Å, radii from Shannon, 1976). Notably, allanite-(La) with an excess of V^{3+} , Fe^{2+} and Mn^{2+} is poor in Cr, which could be entirely accommodated at the *M1* site.

Vanadium was probably remobilized by metamorphic processes from the organic matter and

incorporated into silicate minerals (Canet *et al.*, 2003; Uher *et al.*, 2008 and references therein) and the Cr source is probably related to magmatic processes. Torrez-Ruiz *et al.* (2003) suggested the following two origins of the Cr-bearing metamorphic minerals: (1) the activity of Cr-rich hydrothermal fluids produced from the alteration of mafic/ultramafic rocks; and (2) metamorphic reactions inducing the destruction of preexisting Cr-rich phases. However, there is no direct evidence for either of these interpretations in Čierna Lehota, where metamafic rocks could be the source of Cr, but the influence of the hydrothermal processes is not evident. Although, residual chromium minerals such as Cr-spinel were not observed in the samples, these may have been completely decomposed during metamorphism. It is probable that a combination of these processes played a part and moreover, heterogeneity of Cr distribution can result from Cr immobility under metamorphic conditions following chromite decomposition (Nagashima *et al.*, 2006).

One of the characteristic features of the epidote-supergroup minerals studied is the irregular Czo-Muk zone texture (Fig. 2). While developed zones can be attributed mainly to REE variations, there is also a difference in Cr content whereby REE-rich zones are slightly depleted in Cr. These can be interpreted as the product of a metasomatic alteration and dissolution-precipitation process (Putnis, 2002, 2009) by fluids with a high alkali content. A similar phenomenon is observed in secondary domains in garnet where this process could be connected with partial exsolution of a zone richer in REE and poorer in Cr due to lower mobility of Cr during metamorphic processes (Treolar, 1987b; Nagashima *et al.*, 2006).

On the basis of poor X-ray and electron diffraction patterns, Nagashima *et al.* (2011) initially considered that Cr-rich clinozoisite from Finland and Japan resembles metamict epidote-supergroup minerals. However, it does not contain significant U or Th as potential sources of radiation and destruction of lattice periodicity, so consequently they concluded that increased Cr and V content in these samples is due to the presence of a Cr- and V-bearing amorphous phase, which is not part of the clinozoisite structure. Rare-earth-element-dominant epidote-supergroup minerals may also contain an increased Cr content. Consequently, the exsolution of a Cr- and V-bearing amorphous phase presumed in Cr-rich clinozoisite from Finland and Japan (Nagashima *et al.*, 2011) may also result in development of

zones with higher and lower Cr content in our samples, and therefore the zones with a higher proportion of the above-mentioned amorphous phase would have lower REE contents. However, proving, or disproving, each interpretation requires a more detailed analytical approach.

Incorporation of the REE in the epidote-supergroup minerals structure results from complex substitutions involving the 10-coordinated *A2* site and the octahedral *M3* site (Rouse and Peacor, 1993). The REE may be included in the $\text{Fe}^{2+} \text{REEFe}_{-1}^{3+} \text{Ca}_{-1}$ substitution in the epidote–allanite solid solution (Ericit, 2002). This substitution produces an allanite-(La) composition in the epidote-supergroup minerals from Čierna Lehota. More rarely, Mg-dominant dissakisite composition results from $\text{REEMgCa}_{-1}\text{Al}_{-1}$ substitution (Enami and Zang, 1988). Whereas $\text{REEMgCa}_{-1}\text{Cr}_{-1}$ substitution appears to be present in Cr-rich dissakisite from Outokumpu (Treolar and Charnley, 1987) and substitution from Pezinok–Rybníček is $\text{REEMgCa}_{-1}\text{V}_{-1}$ (Bačík and Uher, 2010). Importantly, all these substitutions play a role in variations of the Čierna Lehota epidote-supergroup minerals composition. Enrichment in Mn was also observed in the Aln-Muk zone of the epidote-supergroup minerals studies, and this may result from the combination of $\text{REEMnCa}_{-1}\text{Al}_{-1}$, $\text{REEMnCa}_{-1}\text{V}_{-1}$ and $\text{REEMnCa}_{-1}\text{Cr}_{-1}$ substitutions. Interestingly, Mn decreases in the outer zones of epidote-supergroup minerals crystals. While this can be explained by the chemical properties of younger clinozoisite and mukhinite with distinctly lower REE content, whereby trivalent cations are preferred. It is unlikely that Mn^{3+} is present because of the reducing environment resulting from the presence of organogenic carbon at Čierna Lehota. Moreover, Mn is preferentially incorporated at the 8-coordinated site in garnet relative to epidote-supergroup minerals. This preference is evident in Čierna Lehota garnets because the increased spessartine component can be correlated with the Czo-Muk zone in epidote-supergroup minerals.

However, the sum of typical octahedral cations is higher than 3 apfu in some compositions in the Aln-Muk zone. Although this may be explained by analytical errors, assigning part of the Mn^{2+} to the *A1* site can easily solve the problem. The substitution of Mn for Ca at *A1* is common in allanite-group minerals, resulting in ^{41}Mn -dominant end-members such as manganiandrosite-(La) (Bonazzi *et al.*, 1996) and ferriandrosite-(La) (Nagashima *et al.*, 2015). Moreover, ^{41}Ca -dominant

vanadoallanite-(La) and ferriakasakaite-(La) also contain a significant proportion of ^{41}Mn (Nagashima *et al.*, 2013, 2015).

Evolution of garnet- and epidote-supergroup minerals

The relationship of the silicate minerals investigated to associated minerals is usually difficult to deduce because of the strong tectonic reworking and hydrothermal alteration of the host rock; resulting in the silicate minerals being surrounded and isolated by pyrite (Figs 2, 5). On the basis of textural relationships, we assume that epidote-supergroup minerals, garnets, apatite, Ba-rich feldspar and plagioclase form a primary metamorphic association. These metamorphic minerals are typically overgrown by late chlorite and quartz (Figs 2, 5). Moreover, the younger pyrite, and locally chalcopyrite and sphalerite commonly fill fissures in silicate minerals (Figs 2, 5).

It is difficult to correlate individual epidote-supergroup minerals and garnet compositions to associated minerals but some relationships can be inferred. The Aln-Muk is obviously the oldest generation in epidote-supergroup minerals because it is never isolated but always overgrown by Czo-Muk, and it may represent the first stage of progressive metamorphism. The system of cracks localized only in the epidote-supergroup minerals Aln-Muk core suggests that it was overprinted by tectonic processes before the formation of the Czo-Muk zone. The Czo-Muk zone of epidote-supergroup minerals is synchronous with Gld 2A garnet, as indicated by their close association with well-defined boundaries between grains, but is older than the secondary Grs 2B garnet types that enclose it (Fig. 2d). This also demonstrates that Aln-Muk is older than all the garnet. Apatite and plagioclase probably crystallized contemporaneously with Czo-Muk and are older than Czo (Fig. 5b). However, Czo-Muk is younger than Ba-rich K-feldspar because it forms on the feldspar crystal rim (Fig. 5c), and the youngest Czo probably formed with Grs 2 (Fig. 5e).

The evolution of the mineralization can be compared to the occurrence of V-Cr-rich silicate mineralization in Pezinok–Rybníček, which is analogous to Čierna Lehota in geological position, age, whole-rock composition and metamorphic evolution (Uher *et al.*, 2008; Bačík and Uher, 2010). Enrichment of primary mafic volcanic rocks in specific elements including V, Cr, Fe and Mg is

most probable due to their association with pyrite-pyrrhotite SEDEX mineralization (Uher *et al.*, 2008). Primary rocks can be interpreted as ocean-ridge sedimentary rocks consisting of material from two different sources: altered N-MORB-type basalts; and ocean-floor siliceous sediments with a significant proportion of organic matter (Mérés, 2005).

The compositions of garnets in both the Čierna Lehota and Pezinok–Rybníček occurrences have V-Cr-rich members with a goldmanite–grossular–uvarovite solid solution. As in epidote-supergroup minerals, garnets from the Pezinok area are richer in V and Cr with dominant goldmanite composition and only partly changing to V-(Cr)-rich grossular (Uher *et al.*, 1994, 2008). In contrast, goldmanite is volumetrically a minor phase in Čierna Lehota with lower contents of both V and Cr than in the Pezinok area. Moreover, the Mn content is the main difference between these occurrences – Pezinok V-Cr garnets contain no more than 0.29 Mn apfu (Uher *et al.*, 2008), whereas Mn-rich grossular and spessartine (Grs 2B–Sps 2) in Čierna Lehota contain up to 1.42 Mn apfu (Table 1, Fig. 3a).

The zoning of epidote-supergroup minerals is also very similar to Pezinok–Rybníček with a REE enriched core and a V- and Cr-enriched intermediate zone decreasing to the clinozoisite composition rim (Bačík and Uher, 2010). While this coincidental enrichment in V and Cr is specific for these two localities, there are significant differences in epidote-supergroup minerals from Čierna Lehota and Pezinok–Rybníček. The REE-rich core in Čierna Lehota has mostly an allanite-(La) composition and the dissakisite-(La) component is dominant in only a few places, whereas this component generally dominates at Pezinok–Rybníček (Bačík and Uher, 2010). The intermediate zone in Pezinok–Rybníček is also richer in V and Cr with a significant proportion of the mukhinite component (Bačík and Uher, 2010), while V and Cr contents at Čierna Lehota are lower, resulting in a V- and Cr-bearing clinozoisite generally containing a low proportion of the mukhinite component. Negative Ce anomalies are characteristic of both the studied epidote-supergroup minerals and those from Pezinok–Rybníček (Bačík and Uher, 2010). This may have resulted from interaction between seawater, hydrothermal fluids and basalts with related hyaloclastites on the ocean floor (Mérés, 2005). The enrichment in HREE in the garnets can be attributed to structural requirements which result in a preference for HREE incorporation in garnet (e.g. Grew *et al.*, 2010).

These differences may have been caused by different palaeogeographical positions of the precursors to the two deposits. The mineralization at Pezinok–Rybniček primarily originated from V-, Cr- and C-rich mafic pyroclastic rocks on the deep ocean floor with the sedimentary admixture affected by volcano-exhalative processes (Uher *et al.*, 2008). Abundant pyrite and pyrrhotite produced by volcano-exhalative processes formed disseminated crystals or sulfide-rich stratiform layers and small localized SEDEX-type pyrite deposits in the ‘productive zones’ of the Pezinok–Pernek crystalline complex (Cambel, 1958). Although Čierna Lehota shares similar features, increased Mn content in garnets and Ba in feldspars (Bačík *et al.*, unpublished data) suggest different volcano-exhalative processes. Barium in the form of baryte is typical in volcano-exhalative deposits, and while pyrrhotite- and pyrite-dominant mineralization originating from ‘black smokers’ at temperatures around 350°C contains baryte, larger amounts are produced by ‘white smokers’ at temperatures <300°C (Pirajno, 1992, 2009). Moreover, baryte is widely disseminated in ocean-floor sediments where it is related to strong upwelling and high productivity on continental margins (Koski and Hein, 2003). Consequently, although it is impossible to determine the origin of Mn and Ba on the basis of current data, their increased content at the Čierna Lehota deposit suggests that the protolith may have derived from an area further from the ocean ridge than the Pezinok–Rybniček protolith.

Regardless of all these differences, the multi-stage evolution of epidote-supergroup minerals and garnets is similar at both localities due to very similar geological settings. The early Variscan, low-grade greenschist-facies metamorphism observed in Pezinok–Rybniček, which resulted in a fine-grained silicate + carbonaceous matter + pyrite mineral assemblage in the mafic tuffs and metamorphic foliation (Uher *et al.*, 2008), is hard to see in the Čierna Lehota epidote-supergroup minerals and garnets, and therefore we question whether the early Variscan metamorphism affected Čierna Lehota. However, the Aln-Muk cores in epidote-supergroup minerals could have formed either during this stage or be a product of pre-Variscan volcanic processes. The development of V- and Cr-rich zones in both garnets (Grs 1) and epidote-supergroup minerals (Czo-Muk) could have resulted from late-Variscan contact metamorphism associated with the granite intrusion in the Suchý Massif. The situation is analogous to the

development of epidote-supergroup minerals and garnets with similar compositions at Pezinok–Rybniček, where minerals with this composition formed coevally with the intrusion of granitoid in the Modra Massif (Uher *et al.*, 2008; Bačík and Uher, 2010). The decrease in temperature after the metamorphic peak resulted in a fluid-driven metasomatic overprint of primary metamorphic assemblage and formation of the REE-, V- and Cr-poor Czo epidote-supergroup-mineral zone and secondary garnet types (Gld 2A and 2B, Grs 2A and 2B, Sps 2). (3) The last stage highlights the differences between the two localities. The later and probable Alpine metamorphic association in Pezinok–Rybniček includes V- and Cr-free clinzoisite (Bačík and Uher, 2010). However, this composition was not observed in Čierna Lehota, where the Czo zone can be correlated to the Czo1 rim in Pezinok–Rybniček (Bačík and Uher, 2010). Therefore, the presence of chlorite on the rims of epidote-supergroup minerals and garnet crystals (Figs 2 and 5) in Čierna Lehota can be attributed either to the final low-T stage of retrograde metamorphic phase or to the Alpine low-temperature hydrothermal overprint.

Acknowledgements

We thank Patrik Konečný, Viera Kolárová and Ivan Holický, for assistance during the EMPA study, and Ray Marshall for the review of English language. We also thank the editors of *Mineralogical Magazine* and Masahide Akasaka and the anonymous reviewer for their detailed reviews which improved the quality of our work. This work was supported by the Slovak Research and Development Agency under the contracts APVV-14-0278, APVV-15-0050 and APVV-0081-10, and the Ministry of Education of Slovak Republic grant agency under the contracts VEGA-1/0079/15 and VEGA-1/0499/16.

References

- Anders, E. and Grevesse, N. (1989) Abundances of the elements: Meteoritic and solar. *Geochimica et Cosmochimica Acta*, **53**, 197–214.
- Armbruster, T., Bonazzi, P., Akasaka, M., Bermanec, V., Chopin, C., Gieré, R., Heuss-Assbichler, S., Liebscher, A., Menchetti, S., Pan, Y. and Pasero, M. (2006) Recommended nomenclature of epidote-group minerals. *European Journal of Mineralogy*, **18**, 551–567.
- Bačík, P. and Uher, P. (2010) Dissakisite-(La), mukhinitite, and clinzoisite: V,Cr,REE-rich members of the

- epidote group in amphibole-pyrite-pyrrhotite metabasic rocks from Pezinok, Rybníček mine, Western Carpathians, Slovakia. *Canadian Mineralogist*, **48**, 523–536.
- Benkerrou, C. and Fonteilles, M. (1989) Vanadian garnets in calcareous metapelites and skarns at Coat-an Noz, Belle-Isle-en-Terre (Côtes du Nord), France. *American Mineralogist*, **74**, 852–858.
- Bonazzi, P., Menchetti, S. and Reinecke, T. (1996) Solid solution between piemontite and androsite-(La), a new mineral of the epidote group from Andros Island, Greece. *American Mineralogist*, **81**, 735–742.
- Broska, I. and Uher, P. (2001) Whole-rock chemistry and genetic typology of the West-Carpathian Variscan granites. *Geologica Carpathica*, **52**, 79–90.
- Cambel, B. (1958) Contribution to geology of the Pezinok-Pernek crystalline complex. *Acta geologica et geographica Universitatis Comenianae, Geologica*, **1**, 137–166 [in Slovak].
- Canet, C., Alfonso, P., Melgarejo, J.-C. and Jorge, S. (2003) V-rich minerals in contact-metamorphosed Silurian SEDEX deposits in the Poblet area, southwestern Catalonia, Spain. *Canadian Mineralogist*, **41**, 561–579.
- Černý, P., Litochleb, J. and Šrein, V. (1995) Chromian-vanadian garnets from Domoradice near Český Krumlov graphite deposit. *Bulletin mineralogicko-petrologického oddělení Národního muzea v Praze*, **3**, 205–209 [in Czech].
- Dollase, W.A. (1968) Refinement and comparison of the structures of zoisite and clinozoisite. *American Mineralogist*, **53**, 1882–1898.
- Dyda, M. (1994) Geothermobarometric characteristics of some Tatric crystalline basement Units (Western Carpathians). *Mitteilungen der Österreichischen Geologischen Gesellschaft*, **86**, 45–59.
- Enami, M. and Zang, Q. (1988) Magnesian staurolite in garnet-corundum rocks and eclogite from the Donghai district, Jiangsu province, east China. *American Mineralogist*, **73**, 48–56.
- Ercit, T.S. (2002) The mess that is allanite. *Canadian Mineralogist*, **40**, 1411–1419.
- Filippovskaya, T.B., Shevnin, A.N. and Dubakina, L.S. (1972) Vanadian garnets and hydrogarnets from Lower Paleozoic carbon- and silica-rich schists of Ishimskaya Luka (Northern Kazakhstan). *Doklady Akademii Nauk SSSR, Earth Science Section*, **203**, 1173–1176 [in Russian].
- Finger, F., Broska, I., Haunschmid, B., Hraško, L., Kohút, M., Krenn, E., Petřík, I., Riegler, G. and Uher, P. (2003) Electron-microprobe dating of monazites from Western Carpathian basement granitoids: Plutonic evidence for an important Permian rifting event subsequent to Variscan crustal anatexis. *International Journal of Earth Sciences*, **92**, 86–98.
- Gieré, R. and Sorensen, S. (2004) Allanite and other REE-rich epidote-group minerals. *Reviews in Mineralogy and Geochemistry*, **56**, 431–494.
- Grew, E.S., Marsh, J.H., Yates, M.G., Lazic, B., Ambruster, T., Locock, A.J., Bell, S.W., Dyar, M.D., Bernhardt, H.-J. and Medenbach, O. (2010) Menzerite-(Y), a new garnet species, $\{(Y,REE)(Ca,Fe^{2+})_2\}[(Mg,Fe^{2+})(Fe^{3+},Al)](Si_3)O_{12}$, from a felsic granulite, Parry Sound, Ontario, and a new garnet end-member, $\{Y_2Ca\}[Mg_2](Si_3)O_{12}$. *Canadian Mineralogist*, **48**, 1171–1193.
- Grew, E.S., Locock, A.J., Mills, S.J., Galuskina, I.O., Galuskin, E.V. and Hälenius, U. (2013) Nomenclature of the garnet supergroup. *American Mineralogist*, **98**, 785–811.
- Hovorka, D. and Fejdi, P. (1983) Garnets of peraluminous granites of the Suchý and Malá Magura Mts. (the Western Carpathians) their origin and petrological significance. *Geologický zborník – Geologica Carpathica*, **34**, 103–115.
- Hovorka, D. and Méres, Š. (1991) Pre-Upper Carboniferous gneisses of the Strážovské vrchy Upland and the Malá Fatra Mts. (the Western Carpathians). *Acta Geologica et Geographica Universitatis Comenianae, Geologica*, **46**, 103–169.
- Hrouda, F., Kahan, S. and Putiš, M. (1983) The magnetic and mesoscopic fabrics of the crystalline complex of the Strážovské vrchy Mts. and their tectonic implications. *Geologica Carpathica*, **34**, 717–731.
- Ivan, P. and Méres, Š. (2015) Geochemistry of amphibolites and related graphitic gneisses from the Suchý and Malá Magura Mountains (central Western Carpathians) – evidence for relics of the Variscan ophiolite complex, *Geologica Carpathica*, **66**, 347–360.
- Jeong, G.Y. and Kim, Y.H. (1999) Goldmanite from the black slates of the Ogcheon belt, Korea. *Mineralogical Magazine*, **63**, 253–256.
- Kahan, Š. (1979) Geologic profiles across crystalline complexes of the Strážovské vrchy Hills (Suchý a Malá Magura Mts.). Pp. 153–160 in: *Tectonic profiles across the Západné Karpaty Mts* (M. Maheľ, editor). Dionýz Štúr Geological Institute, Bratislava.
- Kahan, Š. (1980) Strukturelle und metamorphe Charakteristik des Kristallins des Gebirges Strážovské vrchy (Suchý und Malá Magura). *Geologický zborník – Geologica Carpathica*, **31**, 577–601.
- Karev, M.E. (1974) New finds of vanadium-containing minerals in metamorphic rocks of the Kuznetsk Alatau. *Geologiya i Geofizika*, **11**, 141–143 [in Russian].
- Kato, A., Shimizu, M., Okada, Y., Komuro, Y. and Takeda, K. (1994) Vanadium-bearing spessartine and allanite in the manganese-iron ore from the Odaki orebody of the Kyurazawa mine, Ashio Town, Tochigi

- Prefecture, Japan. *Bulletin of the National Science Museum, Tokyo, Series C*, **20**, 1–12.
- Konečný, P., Siman, P., Holický, I., Janák, M. and Kollárová, V. (2004) Method of monazite dating by means of the microprobe. *Mineralia Slovaca*, **36**, 225–235.
- Korikovskiy, S.P., Cambel, B., Mikláš, J. and Janák, M. (1984) Metamorphism of the Malé Karpaty crystalline complex: Stages, zonality, relationship to granitic rocks. *Geologický zborník – Geologica Carpathica*, **35**, 437–462 [in Russian].
- Koski, R.A. and Hein, J.R. (2003) Stratiform barite deposits in the Roberts Mountains allochthon, Nevada: a review of potential analogs in modern sea-floor environments. Pp. 1–17 in: *Contributions to Industrial Minerals Research*. (J.D. Bliss, P.R. Moyle and K.R. Long, editors). U.S. Geological Survey Bulletin 2209-H.
- Kráľ, J., Hess, C., Kober, B. and Lippolt, H.J. (1997) $^{207}\text{Pb}/^{206}\text{Pb}$ and $^{40}\text{Ar}/^{39}\text{Ar}$ age data from plutonic rocks of the Strážovské vrchy Mts. basement, Western Carpathians. Pp. 253–260 in: *Geological Evolution of the Western Carpathians* (P. Grecula, D. Hovorka and M. Putiš, editors). Mineralia Slovaca Monograph, Bratislava.
- Krist, E., Korikovskij, S.P., Putiš, M., Janák, M. and Faryad, S.W. (1992) *Geology and Petrology of Metamorphic Rocks of the Western Carpathian Crystalline Complex*. Comenius University Press, Bratislava, 324 pp.
- Litochleb, J., Novická, Z. and Burda, J. (1985) Vanadian garnets in Proterozoic metasilicites from Struhadlo near Klatovy. *Časopis Národního Muzea Řada Přírodovědná*, **151**, 31–34 [in Czech].
- Litochleb, J., Sejkora, J. and Šrein, V. (1997) Vanadian garnets from Český Krumlov–Městský vrch graphite deposit. *Bulletin mineralogicko-petrologického oddělení Národního muzea v Praze*, **4–5**, 159–160 [in Czech].
- Mahel', M. (1986) *Geological structure of the Czechoslovakian Carpathians. 1. Palealpine units*. Veda, Bratislava, 503 pp. [in Slovak].
- Mahel', M., Kahan, Š., Gross, P., Vaškovský, I. and Salaj, J. (1982) *Geological map of the Strážovské vrchy Hills*, 1: 50,000. Dionýz Štúr Geological Institute, Bratislava.
- Makrygina, V.A., Petrova, Z.I., Koneva, A.A. and Suvorova, L.F. (2004) Finding of Cr-V-containing minerals in marbles and quartzites of the Svyatoi Nos Peninsula (Lake Baikal). *Russian Geology and Geophysics*, **45**, 1441–1449.
- Matsubara, S., Miyawaki, R., Yokoyama, K., Shigeoka, M., Miyajima, H., Suzuki, Y., Murakami, O. and Ishibashi, T. (2010) Momoiite and nagashialite from the Tanohata mine, Iwate Prefecture, Japan. *Bulletin of the National Science Museum, Tokyo, Series C*, **36**, 1–6.
- Méres, Š. (2005) Major, trace element and REE geochemistry of the metamorphosed sedimentary rocks from the Malé Karpaty Mts. (Western Carpathians, Slovak Republic): an implication for sedimentary and metamorphic processes. *Slovak Geological Magazine*, **11**, 107–122.
- Mikuš, T., Chovan, M., Ponomarenko, O., Bondarenko, S. and Grinchenko, O. (2013) Hydrothermal nickel mineralization from the black shales in Čierna Lehota (Western Carpathians, Slovakia). *Mineralogicheskii Zhurnal (Ukraine)*, **35**, 27–32.
- Moench, R.H. and Meyrowitz, R. (1964) Goldmanite, a vanadium garnet from Laguna, New Mexico. *American Mineralogist*, **49**, 644–655.
- Momoi, H. (1964) A new vanadium garnet, $(\text{Mn}, \text{Ca})_3\text{V}_2\text{Si}_3\text{O}_{12}$, from the Yamato Mine, Anami Islands, Japan. *Memoirs of the Faculty of Science Kyushu University, Series D, Geology*, **15**, 73–78.
- Nagashima, M., Akasaka, M. and Sakurai, T. (2006) Chromian epidote in omphacite rocks from the Sambagawa metamorphic belt, central Shikoku, Japan. *Journal of Mineralogical and Petrological Sciences*, **101**, 157–169.
- Nagashima, M., Akasaka, M., Kyono, A., Makino, K. and Ikeda, K. (2007) Distribution of chromium among the octahedral sites in chromian epidote from Iratsu, central Shikoku, Japan. *Journal of Mineralogical and Petrological Sciences*, **102**, 240–254.
- Nagashima, M., Armbruster, T., Herwegh, M., Pettke, T., Lahti, S. and Grobety, B. (2011) Severe structural damage in Cr- and V-rich clinzoisite: relics of an epidote-group mineral with $\text{Ca}_2\text{Al}_2\text{Cr}^{3+}\text{Si}_3\text{O}_{12}(\text{OH})$ composition? *European Journal of Mineralogy*, **23**, 731–743.
- Nagashima, M., Nishio-Hamane, D., Tomita, N., Minakawa, T. and Inaba, S. (2013) Vanadoallanite-(La): a new epidote-supergroup mineral from Ise, Mie Prefecture, Japan. *Mineralogical Magazine*, **77**, 2739–2752.
- Nagashima, M., Nishio-Hamane, D., Tomita, N., Minakawa, T. and Inaba, S. (2015) Ferriakasaite-(La) and ferriandrosite-(La): new epidote-supergroup minerals from Ise, Mie Prefecture, Japan. *Mineralogical Magazine*, **79**, 735–754.
- Osanai, Y., Ueno, T., Tsuchiya, N., Takahashi, Y., Tainosho, Y. and Shiraishi, K. (1990) Finding of vanadium-bearing garnet from the Sor Rondane Mountains, East Africa. *The Antarctic Record*, **34**, 279–291.
- Ovchinnikov, L.N. and Tzimbalko, M.N. (1948) Manganorthite from Vishnevy Mts. *Doklady Akademii Nauk SSSR*, **63**, 191–194 [in Russian].
- Pan, Y. and Fleet, M.E. (1991) Vanadian allanite-(La) and nagashialite-(Ce) from the Hemlo gold deposit, Ontario, Canada. *Mineralogical Magazine*, **55**, 497–507.

- Petrík, I., Broska, I., Lipka, J. and Siman, P. (1995) Granitoid allanite-(Ce) substitution relations, redox conditions and REE distributions (on an example of I-type granitoids, Western Carpathians, Slovakia). *Geologica Carpathica*, **46**, 79–94.
- Pirajno, F. (1992) *Hydrothermal Mineral Deposits: Principles and Fundamental Concepts for the Exploration Geologist*. Springer-Verlag, Berlin, 709 pp.
- Pirajno, F. (2009) *Hydrothermal Processes and Mineral Systems*. Springer-Verlag, Berlin, 1250 pp.
- Plašienka, D., Grecula, P., Putiš, M., Kováč, M. and Hovorka, D. (1997) Evolution and structure of the Western Carpathians: an overview. Pp. 1–24 in: *Geological Evolution of the Western Carpathians* (P. Grecula, D. Hovorka and M. Putiš, editors). Mineralia Slovaca Monograph, Bratislava.
- Pršek, J., Mikuš, T., Makovický, E. and Chovan, M. (2005) Cuprobismutite, kupčíkite, hodrushite and associated sulfosalts from the black shale hosted Ni-Bi-As mineralization at Čierna Lehota, Slovakia. *European Journal of Mineralogy*, **17**, 155–162.
- Putnis, A. (2002) Mineral replacement reactions: from macroscopic observations to microscopic mechanisms. *Mineralogical Magazine*, **66**, 689–708.
- Putnis, A. (2009) Mineral replacement reactions. Pp. 87–124 in: *Thermodynamics and Kinetics of Water-Rock Interactions* (E.H. Oelkers and J. Schott, editors). Reviews in Mineralogy & Geochemistry, **70**. Mineralogical Society of America and The Geochemical Society, Washington DC.
- Rao, A.T. and Babu, V.R.R.M., (1978) Allanite in charnockites from Air Port Hill, Visakhapatnam, Andhra Pradesh, India. *American Mineralogist*, **63**, 330–331.
- Rouse, R.C. and Peacor, D.R. (1993) The crystal structure of dissakisite-(Ce), the Mg analogue of allanite-(Ce). *Canadian Mineralogist*, **31**, 153–157.
- Secco, L., Martignaco, F., Dal Negro, A., Reznitskii, L.Z. and Sklyarov, E.V. (2002) Crystal chemistry of Cr³⁺-V³⁺-rich clinopyroxenes. *American Mineralogist*, **87**, 709–714.
- Shannon, R.D. (1976) Revised effective ionic radii and systematic studies of interatomic distances in halides and chalcogenides. *Acta Crystallographica*, **A32**, 751–767.
- Shepel, A.V. and Karpenko, M.V. (1969) Mukhinite, a new vanadium species of epidote. *Doklady Akademii Nauk SSSR*, **185**, 1342–1345 [in Russian].
- Tanaka, H., Endo, S., Minakawa, T., Enami, M., Nishio-Hamane, D., Miura, H. and Hagiwara, A. (2010) Momoiite, (Mn²⁺,Ca)₃(V³⁺,Al)₂Si₃O₁₂, a new manganese Vanadium garnet from Japan. *Journal of Mineralogical and Petrological Sciences*, **105**, 92–96.
- Torres-Ruiz, J., Pesquera, A. and López Sánchez-Vizcaíno, V. (2003) Chromian tourmaline and associated Cr-bearing minerals from the Nevado-Filábride Complex (Betic Cordilleras, SE Spain). *Mineralogical Magazine*, **67**, 517–533.
- Treloar, P.J. (1987a) Chromian muscovites and epidotes from Outokumpu, Finland. *Mineralogical Magazine*, **51**, 593–599.
- Treloar, P.J. (1987b) The Cr-minerals of Outokumpu—Their chemistry and significance. *Journal of Petrology*, **28**, 867–886.
- Treloar, P.J. and Charnley, N.R. (1987) Chromian allanite from Outokumpu, Finland. *Canadian Mineralogist*, **25**, 413–418.
- Uher, P., Chovan, M. and Majzlan, J. (1994) Vanadian-chromian garnet in mafic pyroclastic rocks of the Malé Karpaty Mts., Western Carpathians, Slovakia. *Canadian Mineralogist*, **32**, 319–326.
- Uher, P., Kováčik, M., Kubiš, M., Shtukenberg, A. and Ozdín, D. (2008) Metamorphic vanadian-chromian silicate mineralization in carbon-rich amphibole schists from the Malé Karpaty Mountains, Western Carpathians, Slovakia. *American Mineralogist*, **93**, 63–73.
- Uher, P., Ondrejka, M., Bačík, P., Broska, I. and Konečný, P. (2015) Britholite, monazite, REE carbonates, and calcite: Products of hydrothermal alteration of allanite and apatite in A-type granite from Stupné, Western Carpathians, Slovakia. *Lithos*, **236–237**, 212–225.
- Vilinovičová, L. (1990) Petrogenesis of gneisses and granitoids from the Strážovské vrchy Mts. *Geologica Carpathica*, **41**, 335–376.
- Yang, J.-J. and Enami, M. (2003) Chromian dissakisite-(Ce) in a garnet lherzolite from the Chinese Su-Lu UHP metamorphic terrane: Implications for Cr incorporation in epidote-group minerals and recycling of REE into the Earth's mantle. *American Mineralogist*, **88**, 604–610.